

Biological Surfaces and their Technological Application - Laboratory and Flight Experiments on Drag Reduction and Separation Control

D.W. Bechert,

DLR, Abt. Turbulenzforschung, Mueller-Breslau-Str. 8, 10623 Berlin, Germany

M. Bruse, W. Hage and R. Meyer,

Herrmann-Föttinger-Institut für Strömungsmechanik, Technische Universität Berlin,
Strasse des 17. Juni 135, 10623 Berlin, Germany

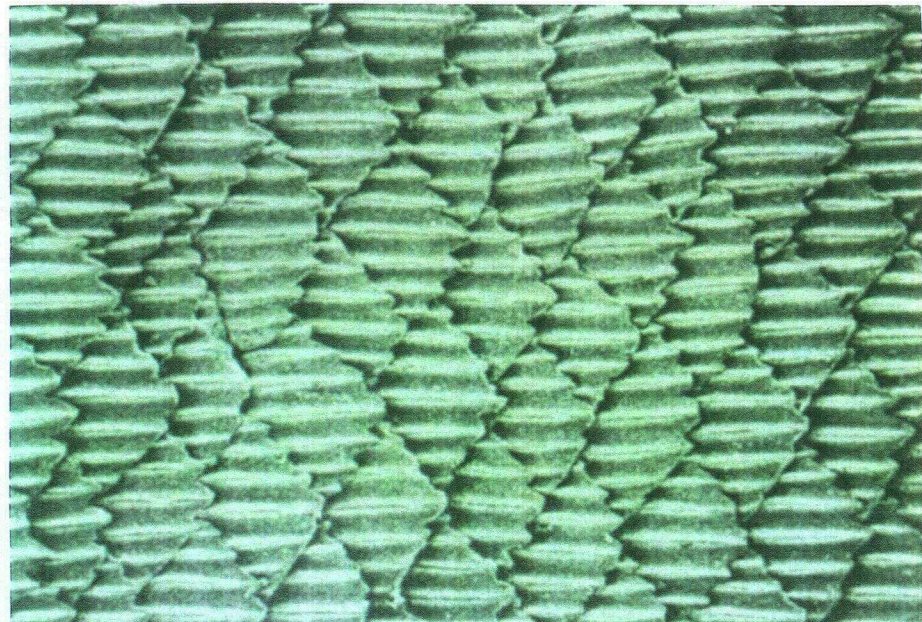
Abstract. A survey is given on fluid dynamical effects caused by structure and properties of biological surfaces. It is demonstrated that the end-product of investigations whose aim is technological applications can also provide insights that help understand biophysical phenomena. The present paper describes techniques for both reducing wall shear stresses and for controlling boundary-layer separation.

(i) Wall shear stress reduction has been investigated experimentally for various riblet surfaces including a shark skin replica. The latter consists of 800 plastic model scales with compliant anchoring. Hairy surfaces are also considered and surfaces where the no-slip condition is modified. Self-cleaning surfaces like the one of lotus leaves represent an interesting option to avoid fluid dynamical deterioration by the agglomeration of dirt. For riblets, two examples of technological implementation are discussed: On long-range commercial aircraft and in gas pipelines.

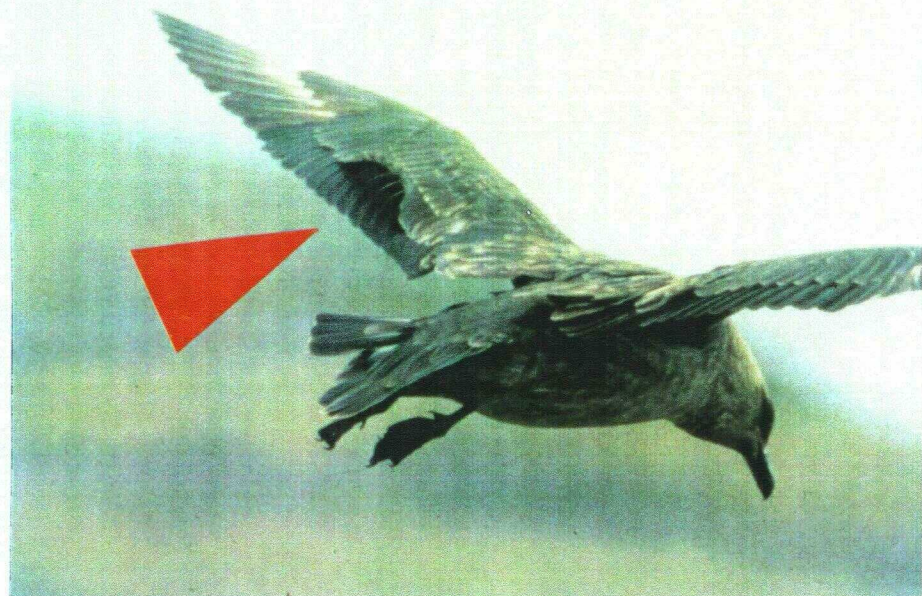
(ii) Separation control is also an important issue in biology. After a few brief comments on vortex generators, two novel mechanisms of separation control by bird feathers are described in detail. Self-activated movable flaps (= artificial bird feathers) represent a high-lift system enhancing the maximum lift of airfoils by about 20 %. This is achieved without perceivable deleterious effects under cruise conditions. Finally, flight experiments with an aircraft with laminar wing and movable flaps are shown.

CONTENTS

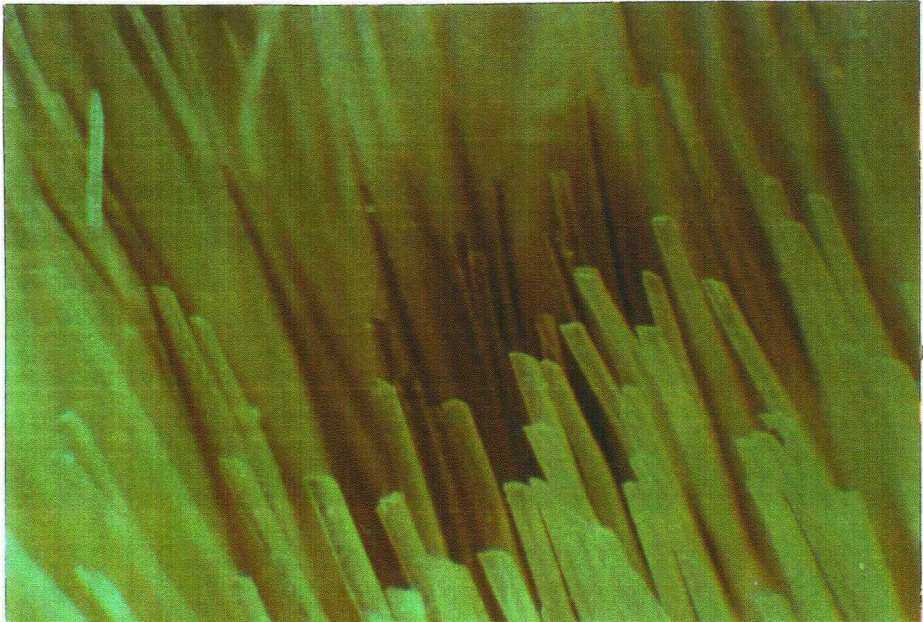
1. INTRODUCTION	3
2. WALL SHEAR STRESS REDUCTION.....	4
2.1 Shark skin or "riblets": The mechanism	4
2.2 "Brother and sister riblets"	7
2.3 Three-dimensional riblets	8
2.4 Experiments with a shark skin replica	12
2.5 Hairy surfaces	16
2.6 Meddling with the no-slip condition.....	18
2.7 Lotus leaves: A self-cleaning system.....	18
2.8 Technological applications I: Aircraft	21
2.9 Technological applications II: Gas pipelines.....	22
3. SEPARATION CONTROL.....	23
3.1 Vortex generators	23
3.2 Movable flaps on wings: Artificial bird feathers.....	27
3.3 Flight experiments with movable flaps.....	34
4. ACKNOWLEDGEMENT	40
5. APPENDIX: COORDINATES OF THE HQ17 AIRFOIL	40
6. REFERENCES	41



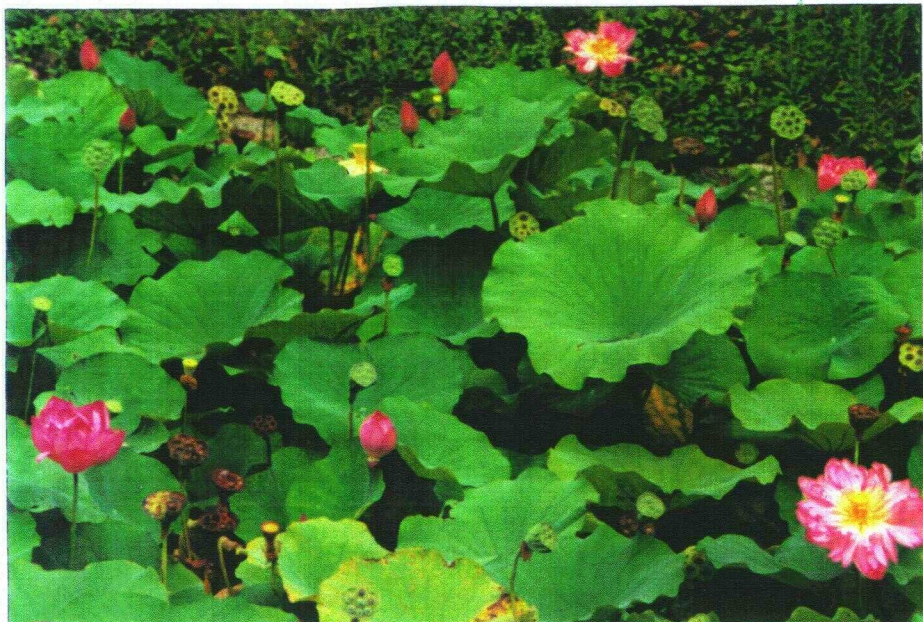
Silky shark skin [1]



Skua wing [2]



Sea leopard skin



Lotus leaves

Figure 1. Biological surfaces with relevant fluid mechanical properties

1. Introduction

Biological surfaces exhibit structures which are, at first sight, both appealing and enigmatic, see Fig. 1. In particular, the skin surfaces of aquatic animals and the feather structure of birds may promise interesting fluid dynamical effects. Often, however, these structures unfold only under the microscope. In other cases, the observation is difficult due to the rapid motion of the animal. In addition, and rather unexpectedly, interesting fluid mechanical properties can be found even on plant surfaces. Besides sheer curiosity, there is an additional scientific motivation for fluid mechanical research related to biology: Natural evolution did proceed according to its own laws and with its own possibilities and limitations. Thus, one can expect that the universal laws of physics are exploited by Nature in an approach unrestricted by the present habits of human thinking. The deviation from the often-treaded alleys of present research could enable us to reap new and useful insights, but access to these insights may be obstructed by the very same present habits of thinking.

One example of such biased perception is to expect only one purpose for a biological surface. By contrast, multiple function is the rule in biology. Consider for instance the mucus on the skin of aquatic animals. It acts as an osmotic barrier against the high salinity of sea water and protects the creature from various kinds of parasites and infections. Since it is also inherently slippery, it helps the animal escape from the grip of a predator. In addition to other useful functions, of which we are not as yet aware, the mucus also operates as a drag reducing agent on some fast predatory fishes, as e.g., barracuda and smallmouth bass [3]. This particular use of mucus enables these predatory fish to attack at increased speed. Once the attack on the prey has been successful, the loss of mucus due to fast swimming, and with it the loss of chemical energy, is compensated for. But the existence of mucus on an aquatic animal does not per se necessarily entail a useful consistency of this mucus for the purpose of drag reduction.

On the other hand, artificial derivatives of fish mucus, i.e., polymer additives for liquids, are used with impressive success in drag reduction technology. For instance, the pumping power required to push crude oil through the Alaska pipeline is very significantly reduced (by about 30 %) by the injection of a few ppm of a gooey substance with only a remote relation to fish mucus [4]. The successful use of this effect clearly demonstrates that one has to understand the physical mechanism at work [5]. By contrast, the direct use of fish slime or its chemical replica would hardly have yielded a suitable oil-soluble additive for crude oil pipe lines. Likewise, it would be naïve to assume that the mere imitation of biology would immediately lead to a technologically viable utilization of the very same effect.

Moreover, some of the concepts which seem to be used by nature still remain tough scientific problems and are only partly understood. One such example is the compliant skin of dolphins. The story started with "Gray's paradox" [6]. Gray suggested a huge gap between the speed of the dolphin and the available (estimated) physiological power of the animal to achieve this speed. Intrigued by this discrepancy, Max Kramer [7] suggested that, due to the compliance of the dolphin skin, it would interact with the water flowing on the body surface in such a way that the flow was stabilized and the transition to turbulence delayed. This delay of the onset of turbulence would in turn dramatically reduce skin friction and drag. Later, theoretical stability calculations supported this idea [8,9]. What followed may be in brief characterized as two decades of both futile and expensive experimental research. Finally, it took the combined effort of first class theoreticians and experimentalists to prove that Kramer's original idea did indeed work as a means to stabilize a laminar boundary layer [10,11].

Apart from the above transition delay mechanism, it has been assumed that dolphin skin also would work under fully turbulent flow conditions. The expected effects are, however, much smaller than those from transition delay and are assumed to amount to only a few percent skin friction reduction [12]. What mechanisms the dolphin really uses is still not clear. The actual margins of dolphin drag reduction are, nevertheless, much smaller than "Gray's paradox" would make one believe. By experiments with trained dolphins, Lang [13] has exposed a crucial deficiency in Gray's considerations: It is not admissible to extrapolate the physiological performance of human athletes to that of dolphins. Dolphins do indeed perform much better, and that eliminates "Gray's paradox." On the other hand, the limited accuracy of Lang's measurements does not eliminate the possibility that

there is some drag reduction being produced by the dolphin skin. Thus, further investigations of this phenomenon could prove fruitful.

This leads to the issue of wishful thinking in conjunction with biological observations. As a matter of fact, drag reduction research usually is motivated by high expectations. The real effects are, however, mostly modest with only a few exceptions, like for instance the influence of polymer additives on turbulent flows. Nevertheless, there is nothing wrong with small improvements, in particular if several of them are used at once. In human technology, aircraft engineers or computer technologists have improved their creations in many small steps to arrive at something which finally appears as a breakthrough. Natural evolution very successfully proceeds in the same way [14,15].

In the present paper, we will focus on two issues:

- (1) Wall friction reduction in turbulent flows caused by surface properties which are related to natural skin structures.
- (2) Separation control devices derived from observations on animals.

Besides discussing bio-fluiddynamical mechanisms, we will also consider technological applications. Eventually, and as a by-product, this leads to a better understanding of the observations one started with. With a few exceptions (e.g., the "lotus mechanism" and the application of riblets in pipelines) we report in the following mostly on own findings. In order to provide a clear distinction between what is confirmed scientifically and what is still a plausible but unconfirmed idea, we label the unconfirmed ideas by *print in italics*. This is because biological research related to engineering applications is pervasively contaminated by wishful thinking. Therefore, we consider it useful to draw a clear line here.

2. Wall shear stress reduction

Drag reduction of a moving animal or vehicle can be achieved by wall shear stress reduction and, in some cases, by separation control. This Section of the paper will mainly focus on turbulent wall shear stress reduction. Obviously, laminar flow offers the lowest attainable wall shear stress. It has been introduced successfully on glider aircraft wings. On commercial aircraft, however, the problems associated with the implementation of laminar flow on swept transonic wings are at present not yet completely solved. Even with laminar flow being maintained on a major percentage of the wings, most of the aircraft surface will still be exposed to turbulent flow. Thus, turbulent wall shear stress reduction is obviously important in all scenarios of future aircraft design. There are, of course, also other important applications of turbulent wall shear stress reduction. One of them is discussed in Section 2.9.

2.1 ***Shark skin or "riblets": The mechanism***

About a decade ago, it had become clear that a turbulent boundary layer on a surface exhibiting longitudinal ribs can develop a lower shear stress than that on a smooth surface [16-18]. Whereas the American scientists invented ribbed surfaces on the basis of fluid-dynamical reasoning, parallel work in Germany was motivated by observations on shark skin [1,18-20]. When we started working in this field, we first confirmed the effect in our wind tunnel using a direct shear force measurement [21]. Subsequently, we developed, together with a group from the University of Naples, a theoretical model [22-24]. This model will be outlined in the following.

The turbulent flow close to a plane smooth wall exhibits very significant instantaneous deviations from the average mean flow direction. Figure 2 shows an instantaneous streamline pattern very close to a smooth wall, as calculated by Spalart and Robinson [25].

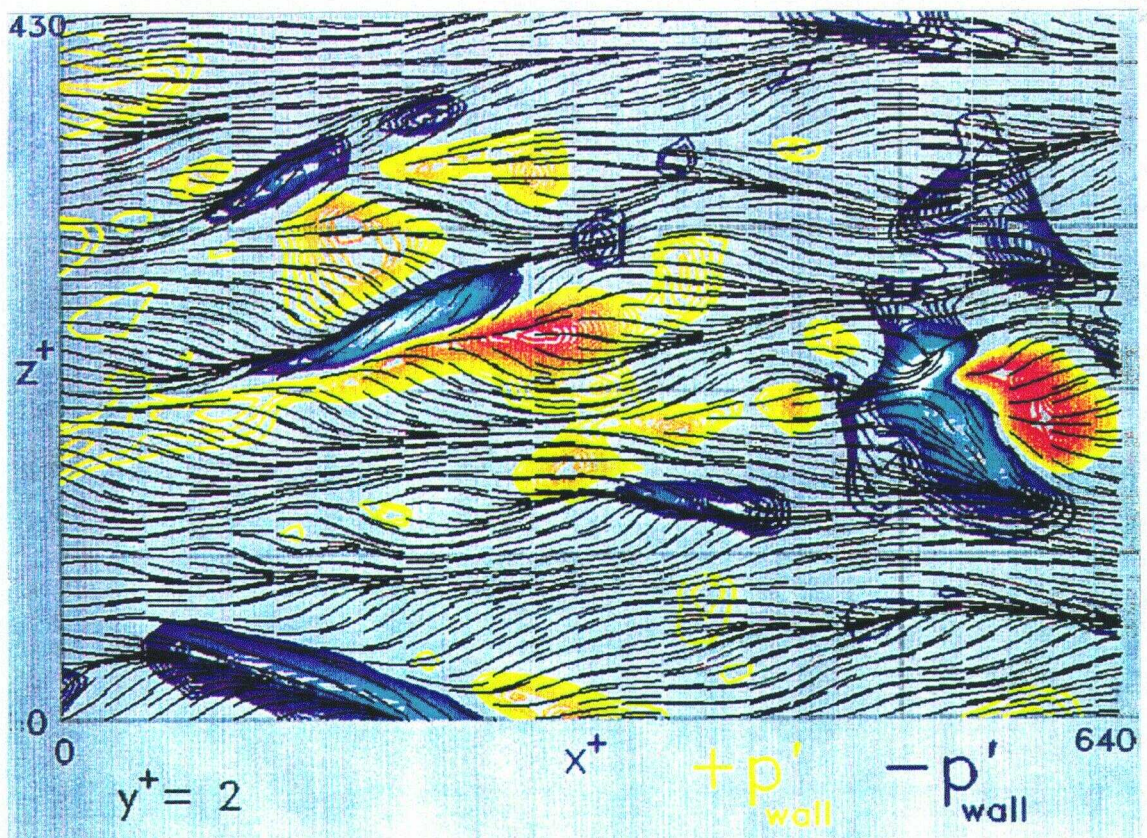


Fig. 2. Instantaneous streamline pattern near a wall [25], at an elevation of $y^+ = 2$, underlaid with contours of wall-pressure. Yellow to red: $p^+ = 3$ to 25. Blue to white: $p^+ = -3$ to -25.

The actual size of the flow regime shown in Fig. 2 would usually be very small. For the water flow on a shark or for the air flow on an aircraft, the actual dimensions of Fig. 2 would be in the millimeter range. In order to obtain generally valid data, quantities are defined in dimensionless wall units. For instance, the distance y perpendicular to the wall takes the form $y^+ = y \cdot u_\tau / v$. This is a Reynolds number defined with the velocity $u_\tau = \sqrt{\tau_0 / \rho}$, where τ_0 is the average wall shear stress. ρ and v are density and kinematic viscosity, defined as usual. In normal circumstances, u_τ assumes a value of a few percent of the free-stream velocity. The streamwise distance x and the lateral length z are nondimensionalized in the same way as y . In Figure 2, instantaneous pressure levels are also given. The pressure is nondimensionalized as $p^+ = p / \tau_0$.

The strong exchange of momentum in a turbulent boundary layer is produced by high speed flow lumps approaching the surface ("sweeps") and by low speed flow moving away from the surface ("ejections") into the high speed regions of the flow, see Fig. 2. Regions of impinging flow ("sweeps") mostly occur in regions of elevated pressure (yellow to red), whereas "ejections", i.e., where the flow moves away from the surface, correspond mostly to regions of lower pressure (blue to white). This exchange of fluid normal to the surface generates the enhanced shear stress of a turbulent flow because high speed flow is decelerated efficiently when it is swept towards the surface. By contrast, such an exchange normal to the surface does not occur in a laminar flow where the streamlines are essentially parallel and the flow lacks such violent local events.

It is also obvious from Figure 2 that local events as "sweeps" and "ejections" require fluid motion in the lateral z -direction. Thus, hampering w -velocities in the z -direction will reduce momentum transfer and skin friction. It is plausible that that can be achieved with ribs on the surface which are aligned in the mean flow direction. On the other hand, it is known that surfaces exhibiting protrusions higher than about $y^+ \approx 5$ do increase the wall shear stress [26]. However, for protrusions

smaller than $y^+ \approx 3-5$, ribs or other roughnesses are imbedded in the viscous sublayer. In this layer, very close to the wall, any fluid behaves like a highly viscous fluid, e.g., like honey. Therefore, it is admissible to calculate the flow around very small ribs with a viscous theory. Under viscous flow conditions, it turns out that the ribbed surface appears as a smooth surface located at a virtual origin, see Figure 3. However, the location of the origin, i.e., its elevation above the groove floor depends on the flow direction. For cross flow on the ribs, the virtual origin is closer to the rib tips than for longitudinal flow. The difference between these two heights we call the "protrusion height difference", Δh . The existence of this difference has interesting consequences: If a flow motion is generated by a fluid lump in a plane at a height y^+ above the surface, the fluid lump experiences a higher resistance if it moves laterally than if it moves in the longitudinal direction. In this way, the cross flow is hampered by the ribs, as desired, and thus ribs do indeed reduce momentum transfer and shear stress.

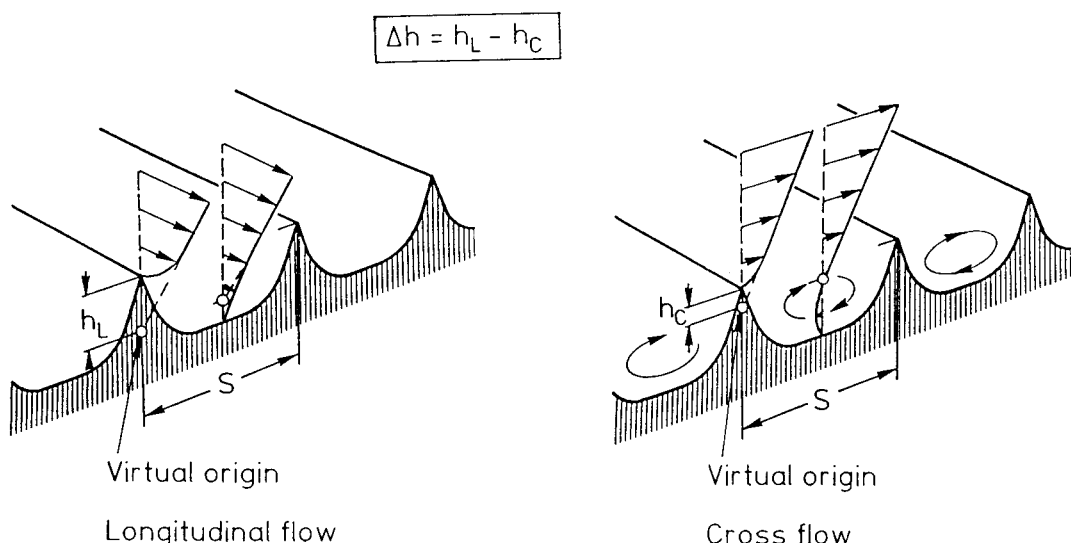


Fig. 3 Longitudinal and cross flow on a ribbed surface

Therefore, for an optimization of the shear stress reduction, we have to select a ribbed surface which exhibits a maximum difference of the virtual origins for longitudinal and cross flow. As the theory shows [24], the maximum height difference is obtained for very thin blade-like ribs. The rib height should be $h \geq 0.6 s$, where s is the lateral rib spacing. For this value of the rib height, the maximum difference of the elevation of the origins, or the protrusion height difference is $\Delta h_{\max} = 0.132 s$. Careful experiments in our oil channel [27] with an adjustable blade rib height [28] have shown that the optimal rib height is actually slightly lower, at $h = 0.50 s$. With this surface, a turbulent shear stress reduction of 9.9 % below that of a smooth surface has been achieved [28]. Figure 4 shows the data of optimal blade rib surfaces as compared to "riblets" with triangular cross-section, which had previously been considered as optimal. Clearly, it is difficult to manufacture surfaces with blade ribs. Therefore, we devised wedge-like ribs which still produce an impressive wall shear stress reduction, see Fig. 4. Ribbed surfaces such as the ones shown in Fig. 4 perform well over a certain s^+ range, which corresponds to a particular velocity range. By selecting an appropriate spacing s of the ribs, one can adjust the ribbed surface to the flow conditions at hand.

In Fig. 4, $\Delta\tau$ is the difference between shear stress τ on the ribbed surface and τ_0 on a smooth reference surface, i.e., $\Delta\tau = \tau - \tau_0$. Negative values of $\Delta\tau/\tau_0$ refer to drag reduction and positive values to an increase of drag.

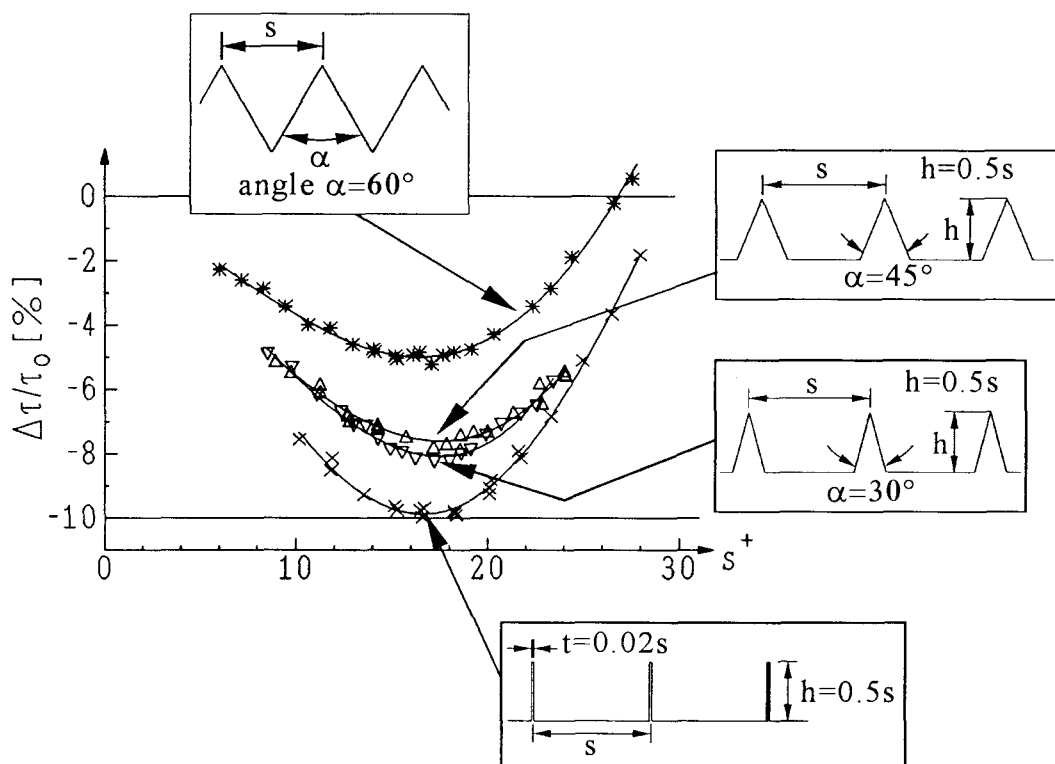


Fig. 4. Drag reduction performance of various rib geometries.

2.2 "Brother and sister ripples"

The viscous theory [22-24,28] appears to provide a useful prediction for an optimal rib height, i.e., $h/s \geq 0.6$. As a guideline for the experiments, this has turned out to be very useful. However, for deeper grooves exceeding $h/s \approx 0.6$, the measured performance deteriorates rapidly, a fact which is not predicted by the simplified viscous theory. This deleterious effect is probably due to increased sloshing of the fluid in the grooves. Sloshing is excited by the fluctuating pressures of the turbulence above the surface. Sloshing entails enhanced momentum transfer and, as a consequence thereof, increased wall shear stress occurs.

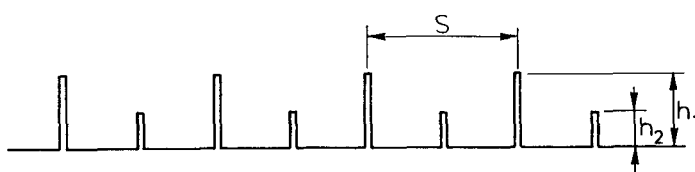


Fig. 5 "Brother & sister ripples"

The above physical description led to the idea that sloshing in the grooves might be reduced by inserting an additional small rib on the floor between the previous ribs. For this arrangement, we have coined the name "brother & sister riblets", see Figure 5. A careful parametric study has been carried out with this configuration [29]. Later, this study was repeated in our laboratory with different hardware and improved data corrections. The result is neither encouraging nor is it disappointing: "Brother & sister" riblets can be as good as the best previous riblets, i.e., blade riblets having uniform height. There is a broad regime of parameters for which the drag reduction remains practically unchanged, with values around and slightly above 9 % [29]. It is conceivable that "brother & sister riblets" may even beat blade riblets by a few tenths of a percent. However, to prove that would not be possible with our present measuring accuracy which is, nevertheless, excellent ($\pm 0.2 \%$).

If there is such a broad range of optimal configurations, we should also see ribs of differing height on real shark skin. Figure 6 shows a photograph of the skin of a white shark [1]. This skin sample exhibits only 3 ribs on each scale (as opposed to the 5 to 7 ribs per scale of other species [1]). In Figure 6 it is clearly visible that the ribs do indeed possess differing height. In addition, the ribs of consecutive scales seem to interlock. Thus, we were curious about this particular feature which leads to the next set of configurations, namely interlocking three-dimensional riblets.



Fig. 6 Scales of the great white shark [1].

2.3 *Three-dimensional riblets*

Observations on shark skin and ideas similar to the ones on "brother & sister riblets" led us to the investigation of 3D-riblets. Thus, we were wondering whether or not interlocking riblets of finite length may be a viable method for turbulent shear stress reduction. For our experiments, we again used thin blades as ribs. The blades were formed by the wire discharge eroding technique to obtain the shape shown in Figure 7. Subsequently, the blades were inserted into an array of slits in a flat plate. Then the blades were locked to a second plate below the slit plate (see Fig. 7). By moving the two plates relative to each other, the rib height h of the blades could be varied during the experiment. We tested 3 different rib lengths of the rib type shown in Figure 7. A photograph of one surface can be seen in Figure 8. Besides the shapes shown in Figures 7 and 8 we also tested ribs with vertical leading and trailing edges, i.e., rectangular shape. The measured wall shear stress data are displayed in some detail in an internal report [30]. The shear stress reduction obtained was 7.3 % with the configuration shown in Figure 7. This falls somewhat short of the 9.9 % which we obtained with straight two-dimensional blade ribs.

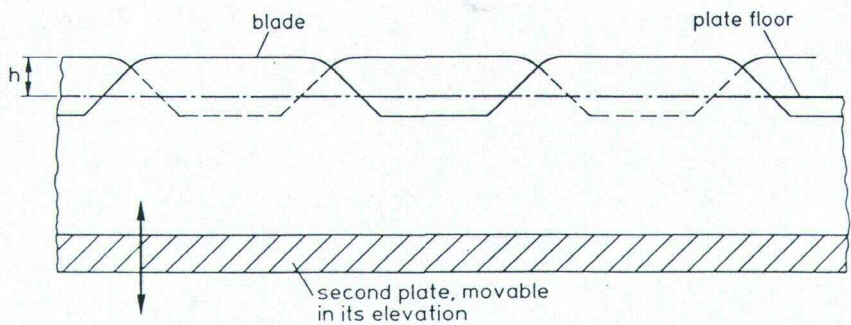


Fig. 7 Shape of the three-dimensional ribs

Recent viscous flow calculations by Luchini & Pozzi [31] have indicated, however, that we may have narrowly missed a more suitable configuration. This configuration would have a slightly wider gap between trailing edge of one rib and leading edge of the next interlocking rib following in the streamwise direction. Thus, there is some hope for a modest improvement. This does not necessarily mean that the data of the best two-dimensional riblets can be exceeded.

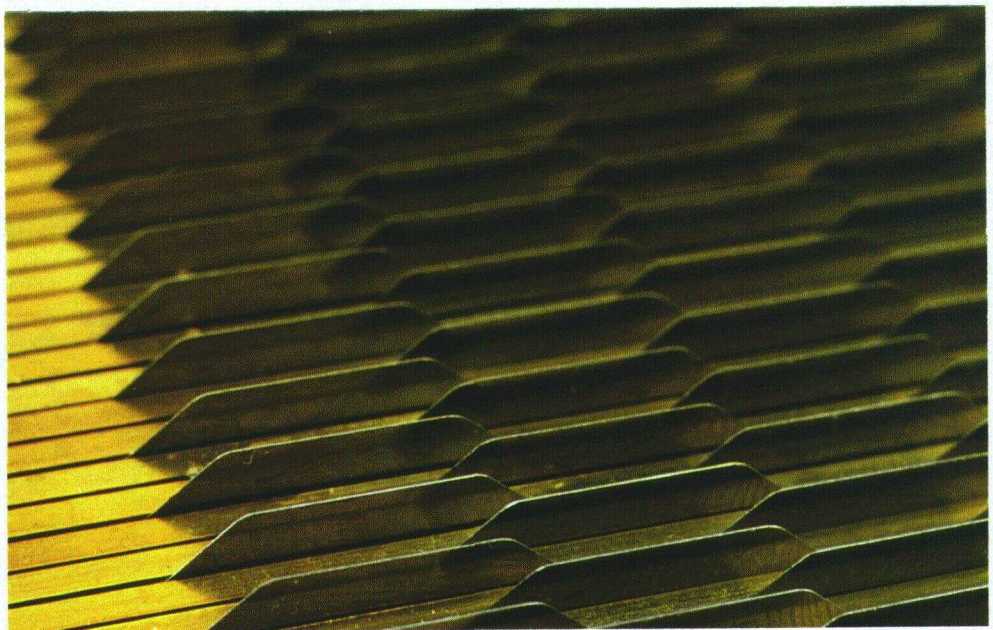


Fig. 8 Photograph of a test surface with three-dimensional ribs.

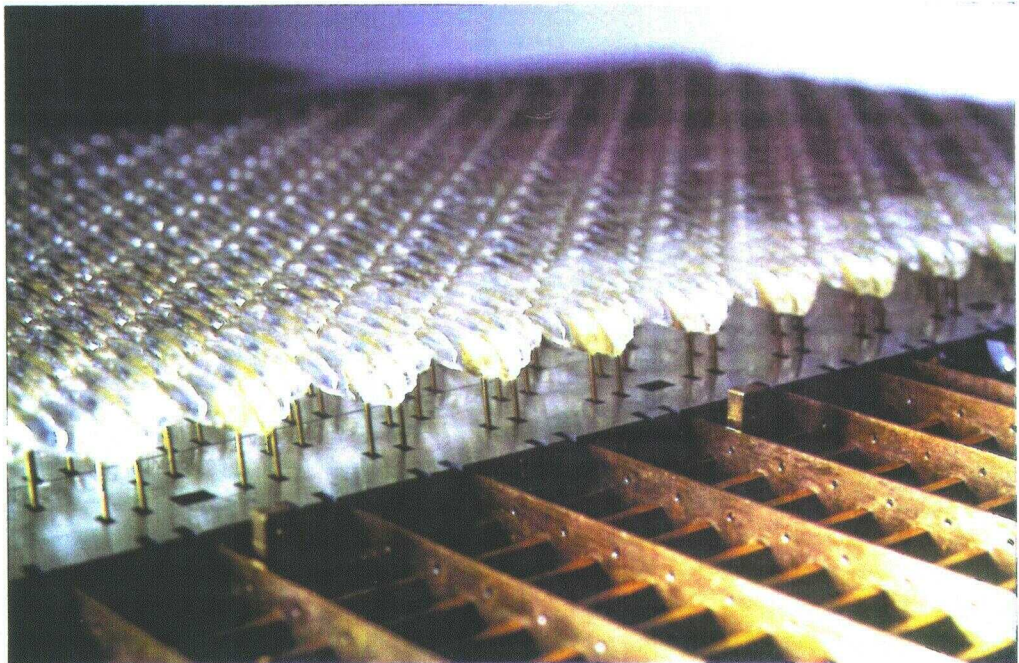


Fig. 9 Photograph of partly assembled shark skin replica

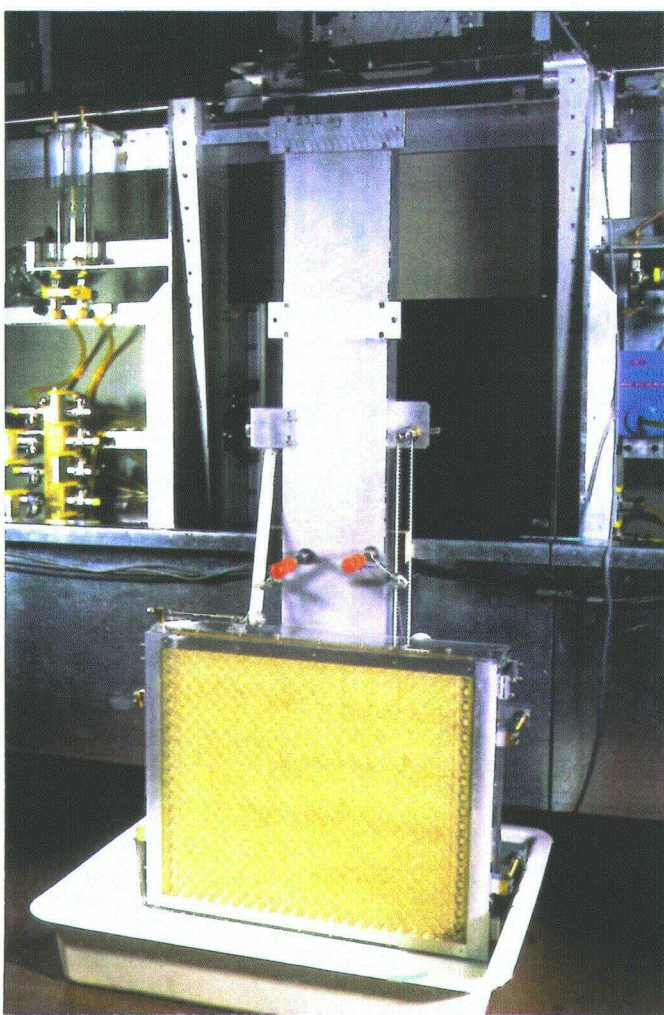


Fig. 10 Test plate with scales before insertion into the oil channel

2.4 Experiments with a shark skin replica

After it had been proved that riblets do indeed work and their shape had been optimized as well as a theory developed, we considered the next crucial question to be: Are there other mechanisms at work on real shark skin? In simplistic terms: Is there any intriguing mechanism at work which may render actual shark skin superior in a novel and impressive way? Our oil channel [27] offered a unique tool to settle this question. By virtue of the viscosity of the oil, it is possible to emulate the microscopic features of actual shark skin in a dimension magnified one hundred times. Therefore, we were able to emulate (i) the detailed shape of typical shark scales, (ii) the flexible anchoring of the individual scales and (iii) a variable angle of attack of the scales with a global adjustment for all scales.

Previous knowledge about this area was scarce. In the first investigation of this kind, Gren [32] had built an array of magnified plastic model scales and collected Laser Doppler data in an oil channel. He was already able to change the angle of attack of the scales. The only (and, as it will turn out, rather minor) criticisms on his previous work were that (i) he used scale models of a slow shark, the spiny dogfish and (ii) his determination of the wall shear stress was an indirect one using velocity measurements above the surface. In addition, he did not have compliant anchoring of his scales. Independently and at about the same time, we had tried to carry out wind tunnel experiments with a similar aim [21]. Plastic surfaces with a large number of tiny emulated shark scales were built and subsequently tested on a shear stress balance [21]. The various cast plastic surfaces exhibited scales with different angles of attack. The limitations for these latter experiments consisted of (i) a rather poor quality of the artificial shark scale pattern due to imperfections in the microscopic production process, and (ii) that the surface was again rigid, and (iii) that the gaps between the scales were not modeled, which do occur in particular at higher angles of attack. In both previous investigations, however, the finding was identical: At higher angles of attack of the scales the wall shear stress increased dramatically. Only at zero angle with an almost riblet-type surface could one hope for a very modest wall shear stress reduction.

The prospect to carry out new experiments with scales with compliant anchoring, however, was most intriguing. Excited by high expectations, we went through the chore to build a surface with 800 individually movable scales which, on the other hand, could be adjusted globally to different angles of attack, see Figures 9 and 10. The anchoring of the individual scales was achieved by a mechanism which is displayed in Figure 11.

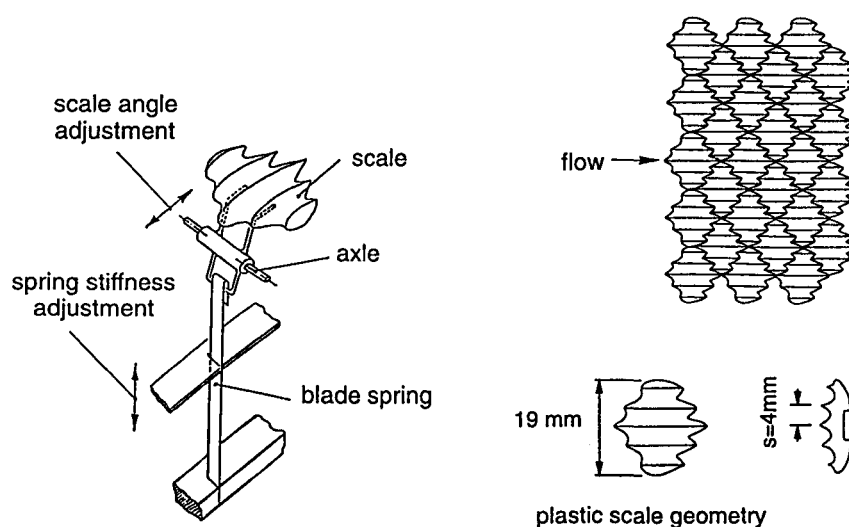


Fig. 11 Schematic of the artificial shark scale arrangement and the suspension mechanism.

By blade springs with variable clamping conditions, the degree of softness of the suspension could be changed. Between "hard" and "soft" suspension, the spring constant could be varied over 3 decades, a feature which was achieved with two sets of blade springs. In Figure 11, a schematic of a plastic scale with 5 ribs can be seen which was designed according to our own microscope observations of hammerhead shark scales. The manufacturing process consisted first of a 600:1 hand-sculptured clay model. From that model, a negative mould was cast. With a pantograph-copy milling machine, the mould was reduced in size to a 100:1 scale. This mould was inserted into a plastic casting machine and 800 polystyrene scales were subsequently produced. In addition, tiny brass wire legs and the other parts of the suspension mechanism were manufactured using suitable tools, then soldered together and glued onto the scales. The scale array can be seen partly assembled and completely assembled in Figures 9 and 10, respectively. Note that suspension stiffness as well as scale angle can be varied during the measurement by remote tooth belt operation.

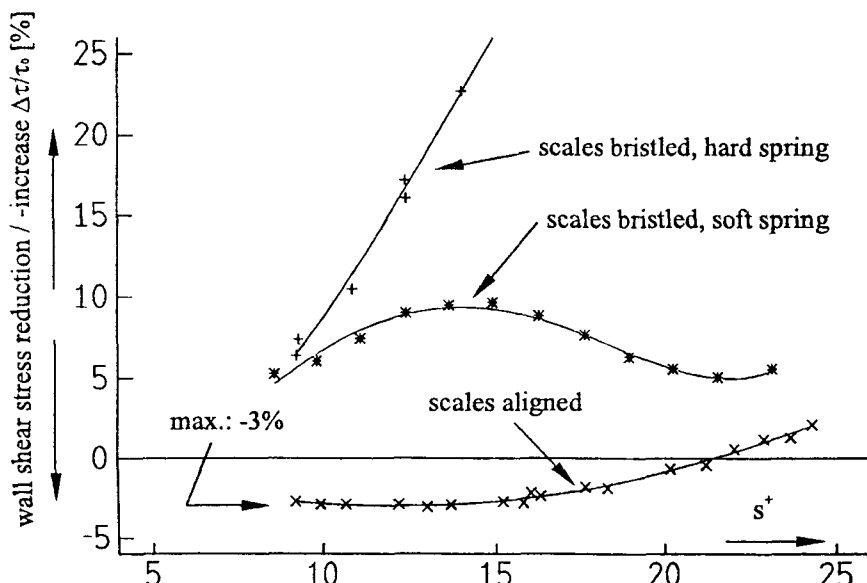


Fig. 12 Typical wall shear stress data of artificial shark scales

A few typical wall shear stress data as measured on our artificial shark scale surface can be seen in Figure 12. For high spring stiffness and with bristled scales the data are consistent with previous results [21,32]. On the other hand, if the scales are not bristled but well aligned so that the scales interlock and leave almost no gaps, we find a modest amount of shear stress reduction (3%). This is when shark scales operate as "riblets". The comparatively modest performance may be due to the residual tiny gaps between the scales and other imperfections. By the way, this is the first time that shear stress reduction has been measured on a shark skin replica. An interesting situation arises when the scales are anchored with a soft mounting. In this case, observations in the oil-channel showed that the scales undergo collective erratic motion in the locally varying instantaneous shear stresses within the turbulent boundary layer. Nevertheless, the curve for soft spring suspension in Figure 12 can still be explained with quasi-static considerations. Incidentally, for aligned scales, there is no difference between rigid and soft suspension. For the aligned condition, the scales actually do have mechanical contact and the surface is indeed rigid, even for the soft suspension. Consider the curve for the soft spring suspension in Figure 12. For bristled scales at low s^+ , i.e., at low velocity and low shear stress, the scales remain bristled and again behave like a stiff and rough surface. However, for increasing s^+ , velocity and shear stress increase. As a consequence thereof, the scales are bent in the streamwise direction and thus the curve approaches the aligned case. This results in a lower friction coefficient c_f and hence the surface behaves more like a smooth surface.

We summarize these data with the statement that, even with a detailed and compliant shark skin replica, we did not find a striking effect, at least as far as shear stress reduction is concerned. As a matter of fact, our synthetic two-dimensional blade rib surfaces do perform significantly better than our ambitious shark skin replica. *There remains, however, the possibility that actual shark skin, say, of a silky shark with its very regular ribs [1], may perform better and indeed closer to our optimized synthetic two-dimensional riblets.*

On the other hand, the data on the softly suspended scales provide some material for further speculations: A shark does not move in a straight line and does not have a rigid body as does a ship. Actually, a shark wiggles a lot. Therefore, the flow conditions on the body and the fins vary periodically and considerably with time. In addition, agility is an important prerequisite for survival. Consequently, separation control may be more important than shear stress reduction. Consider a situation approaching flow separation: For attached flow, the wall shear stress is high. This would refer to a high s^+ in Fig. 12, upper curve, trough regime. However, close to separation, the wall shear stress will be reduced, corresponding to a lower s^+ . With low spring stiffness, the scales would then bristle. They would operate as vortex generators enhancing the mixing in the boundary layer. This would help to keep the flow attached. Maintaining attached flow reduces the overall drag (in spite of a locally increased shear stress) and permits higher lift generation on the fins. Both features enhance agility and speed. We will discuss separation control more specifically in Section 3 of this paper, but here, it might be worthwhile to draw the attention of the reader to the striking similarity (if not identity) of vortex generators as devised by Wheeler [33] and shark scales [1,34,35] or the skin structure of billfishes [36]. Efficient separation control by these scale-like structures has been demonstrated in several laboratories [37-40].

There are more mechanisms which may come into play: If local flow separation occurs, that will also entail local regimes of flow reversal. Under reversed flow conditions, movable scales will bristle and exert an enormously increased resistance to the reversed flow. From our research on separation control with artificial bird feathers (Section 3) we know that this will indeed hamper flow separation.

It has been suggested previously [41] that mucus also plays an important role on shark skin. One may have doubts about this when one touches a freshly killed shark. A shark skin just feels wet and rough and virtually no slime is found upon inspection of the skin. However, one should be cautious here. Maybe, the shark uses its mucus more efficiently and therefore less visibly. The combination of riblets and polymer additives does indeed work very well. Virk & Koury's data indicate that the combination of riblets and polymer additives actually works better than the algebraic sum of both effects [42]. Due to the strong effect of polymer additives, however, the lateral rib spacing has to be adjusted to the modified flow situation. That entails a wider spacing for the same flow speed or it requires an increased flow speed for the same rib spacing. The latter property would suggest the use of polymer additives only for high-speed emergency situations. This also makes sense in terms of energy conservation, because the use of polymer additives is connected to a loss of chemical energy.

2.5 Hairy surfaces

The first suggestion ever for a drag-reducing surface was contributed by Max Kramer in 1937 [43]. It consists of strings stretched in the streamwise direction above a flat surface. His reasoning was that the shear stress being exerted by the flow would be concentrated on the strings and kept away from the flat surface. Obviously, this is correct, but it is not a consistent scheme for drag reduction for the total surface, including the strings. Nevertheless, our concept of cross flow resistance of riblets (Section 2.1) also applies here. The viscous flow calculations which show this phenomenon have been carried out previously [44,45]. Actually, the fact that on a string, a viscous cross flow generates a higher resistance than a longitudinal flow is well-known. It is at the core of the theory of the locomotion of microorganisms by flagellate motion of their tails [46].

Thus, with the help of previous theory, we could select a suitable geometry for our experiments with stretched strings above a flat plate. Nevertheless, our experimental surface had been equipped with a mechanism by which the height of the strings above the surface could be varied, see Figures 13 and 14. The data from our oil channel experiments can be seen in Figure 14. It is evident that a very modest shear stress reduction can be obtained (1.5 %).

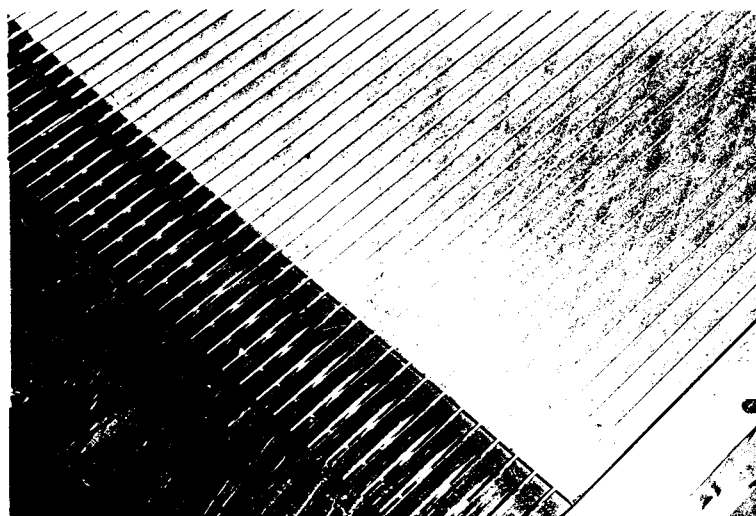


Fig. 13 Test surface with Nylon strings stretched above a flat surface

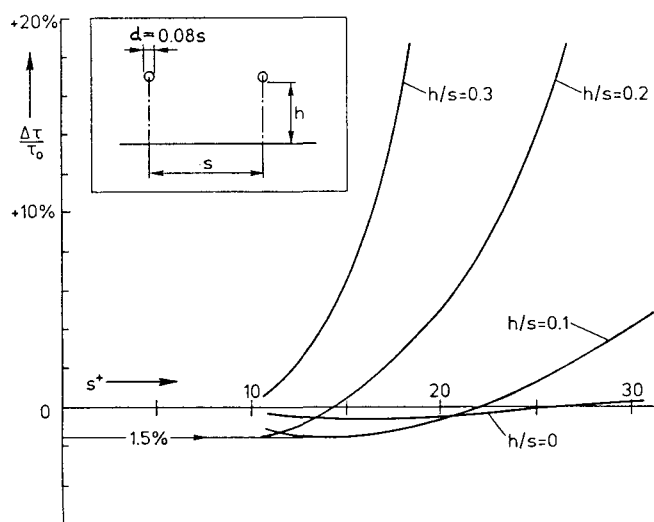


Fig. 14 Test data with a "hairy" surface

At lower string elevations h/s , the strings appear to work similar to riblets. However, at higher string elevations, a disastrous increase of shear stress is found. *We argue that sloshing of fluid underneath the strings in the lateral direction is not sufficiently inhibited by the strings as is the case with riblets.*

Now the question arises whether or not this rather marginal drag reduction mechanism may indeed be utilized by animals moving in water or air. We are not in a position to answer this conclusively, but again we have to remember that biological devices usually serve several purposes

simultaneously. Thus, possibly a marginal drag reduction may be not that relevant here. Other purposes could be much more important. For instance, the very fine and dense fur of otters serves as a heat insulation device, even in water [47]. On the other hand, the coarse fur of a sea leopard exhibits a quite peculiar hair structure (see Figure 1). The cross-section of the comparatively stiff hairs is not round, but flat. As one fluid dynamical purpose of this structure, one may speculate that this type of hair also may inhibit reversed flow and thus may be able to limit flow separation. An (albeit marginal) effect of this kind has been demonstrated for the fur of a certain flying squirrel [48]. A rather obvious purpose, however, is the enhanced ability of sea leopards and seals to move on ice and snow with such a coarse fur. The short length (about 6 mm) and the exceptional stiffness of the hairs do support this latter assumption. Skiers may remember that, before artificial seal fur became available, natural seal fur had been attached underneath the ski during ascent on steep slopes.

2.6 Meddling with the no-slip condition

Usually, one assumes that the fluid on the surface of a moving body assumes the same velocity as the moving body itself. This is what fluid dynamicists call the "no-slip condition". It sets the brackets for the range of fluid dynamical shear stress and drag. There are, however, ways to circumvent this confining condition.

- (i) If the skin is not fixed to the body but can move relative to it, the drag of the body can be reduced. Assume, for instance, that the rigid surface of a body is replaced by a belt which is driven by the shear stress of the flow itself. For this particular case, we have demonstrated experimentally that a reduction of the drag is possible [49].
- (ii) The motion of a spherical oil droplet in water cannot be correctly predicted by Stokes' law for the motion of a rigid sphere in a liquid. This is because the oil inside the droplet takes part in the fluid motion. Therefore, the drag of the liquid droplet is lower than that of the rigid sphere [50].
- (iii) The ejection of air at the surface of a body moving through water efficiently reduces the drag [51]. A recent video documentation of swimming penguins [52] clearly shows that this mechanism is also used in nature: The penguins exhale air before emerging at high speed from the sea. Even more intriguing is the observation [52] that exhaled air sometimes agglomerates in rings around the body of the penguins and remains there for several seconds. *The wavy contour of the penguin body may contribute to the stability of those air rings. For a limited time, exhaled air may thus further reduce the drag of penguins, which is already very low [53].*

2.7 Lotus leaves: a self-cleaning system

The particular cleanliness of the sacred lotus (*nelumbo*) has been already observed early in history. It has caused lotus to become a symbol of purity in Asian religions, a fact which is already documented in Sanskrit writings. Nevertheless, a satisfactory scientific explanation of this cleanliness is a fairly recent achievement by Barthlott and Neinhuis [54,55]. Not quite unexpectedly, the cleaning is caused by rain drops. However, the plant surface is water-repellent. The ability to avoid wetting of the leaves is further enhanced by a rough surface structure exhibiting microscopic wax knobs (see Figures 15 and 16). The way in which dirt particles are removed from the surface can be seen in Figure 17. This self-cleaning "invention" is not restricted to the sacred lotus alone, but is also found on various other plants, among them the well-known garden flower nasturtium (*Tropaeolum majus*, German: Kapuzinerkresse) and even on the surface of insect wings [55].

Without doubt, this self-cleaning ability could be emulated on technological surfaces in order to reduce maintenance. For instance, paints or coatings for cars or buildings based on this principle are conceivable. The cleaning of these novel surfaces works well only when soap or detergents are not used. Consequently, the result is a two-fold beneficial environmental effect: water for cleaning is saved and water pollution is reduced.

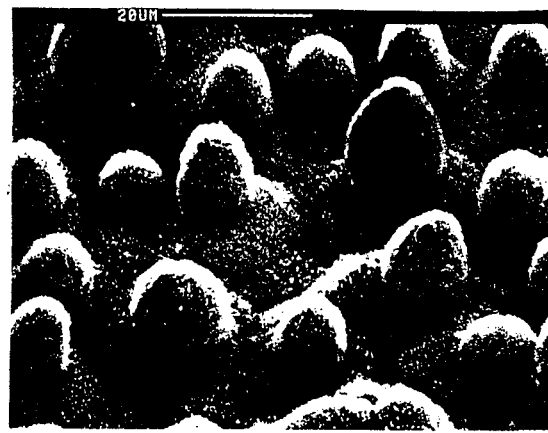


Fig. 15 Micro-structure of lotus leaves [55].

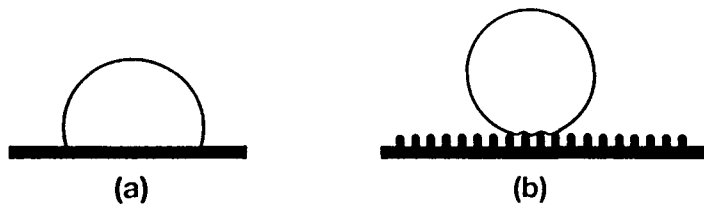


Fig. 16 The effect of the surface structure [54]. Droplet on water-repellent surface (a) and enhanced water repellency caused by surface structure with microscopic knobs (b).

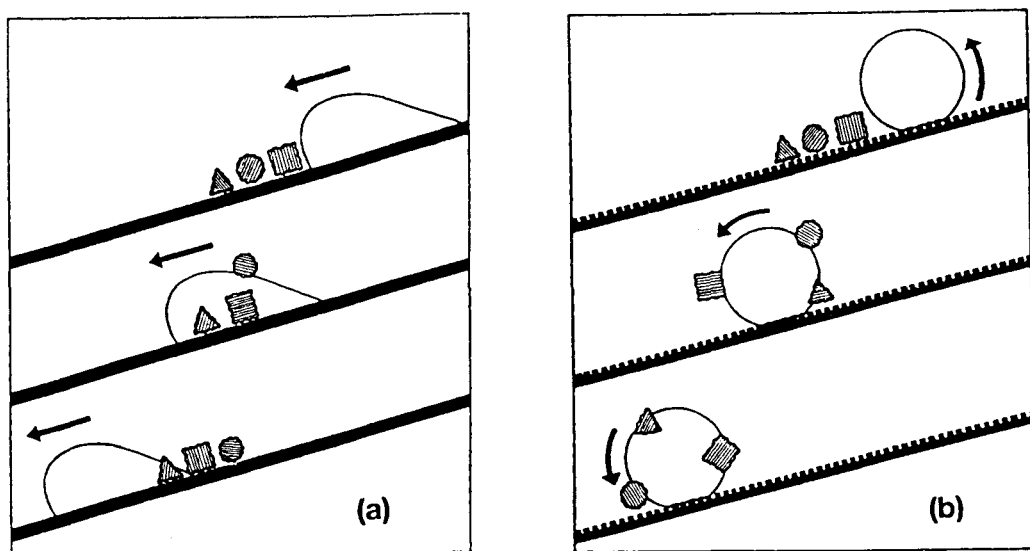


Fig. 17 The self-cleaning mechanism of the lotus plant [55]. On a smooth surface (a) dirt particles are just redistributed by a water droplet. When droplets run off from a rough water-repellent surface (b), dirt particles are removed efficiently.

A water-repellent surface with micro-roughness (with knobs $< 10 \mu$ height) is also an interesting option for laminar wing surfaces on aircraft. A clean and smooth surface is a crucial prerequisite for the proper operation of a laminar wing.

On the other hand, for turbulent shear stress reduction, plastic riblet film is currently used on an Airbus A 340 commercial aircraft (Cathay Pacific Airways). The riblet film being used has a lateral rib spacing of about 60μ . An unexpected, yet preliminary, finding is that this aircraft appears to remain cleaner than others without riblet film. That cleanliness may hint at an inadvertent utilization of the "lotus effect".

On the other hand, and differing from the "lotus effect", the skin of sharks usually appears remarkably clean. Compare, for instance, the skin of whales and whale sharks¹. We speculate that the high local shear stress on the rib tips also may help to prevent dirt particles from settling on the surface. Thus, the initial concerns about an assumed dirt agglomeration on riblet films on aircraft and the ensuing increased maintenance costs may not materialize after all. By contrast, a reduction of maintenance costs by the introduction of new surfaces appears now as a real possibility.

2.8 Technological applications I: Aircraft

At present, artificial shark skin, i.e., riblet film, is on its way to implementation on long-range commercial aircraft. On long-range aircraft (i) the fuel costs contribute perceptively to the direct operating costs and (ii) the fuel weight exceeds by far the payload.

Consider an application on an Airbus A340-300. What are the implications of riblet film to the increase of its economical performance? The contribution of the skin friction to the total drag of this aircraft is about 48 %. This skin friction contribution can be reduced with our optimized riblets with trapezoidal grooves by 8.2 %. If the whole aircraft could be covered with riblet film, that would yield a total drag reduction of the aircraft of about 4 %. However, not the whole surface of the aircraft can be coated with riblet film for various reasons: Dust erosion at the leading edges of the wings and in the vicinity of the landing gear has, over greater time intervals, an effect like sand blasting. In addition, at the leading edges of the wings, the riblet film would interfere with the de-icing system and it would be incompatible with the laminar flow there. Locations where fuel and/or hydraulic fluid may come in contact with the plastic riblet film should also be avoided. Obviously, the windows cannot be covered either. Thus, only about 70 % of the aircraft can be coated with riblet film. In addition, in some places, riblet spacing and alignment will be suboptimal.

On the other hand, some of the roughnesses on the aircraft surface will be covered and thus be smoothened by the film. Moreover, a reduction of the wall friction ensues a slightly thinner boundary layer which, in turn, causes a reduction of the form drag in the rear part of the fuselage. This means that a 3 % reduction in total drag of the aircraft is probably achievable.

The weight of the riblet film is in the order of the weight of the paint which it replaces, i.e., 100-250 kg, depending on the percentage of the surface being covered. Additional technological issues, like durability, UV radiation tolerance, removability of the film, etc., have been solved in the meantime. One particular concern has fed the skepticism of innovation-dreading business people: At present, it takes one week to coat an aircraft with riblet film. During that time, the aircraft earns no money. Plausible as it sounds, it is indeed a spoof argument. Clearly, it is possible to coat the aircraft in steps parallel to other mechanical or maintenance work. By contrast, the perspective of having an aircraft with a dirt-repellent film surface (see Section 2.7) may be an additional attractive item in terms of maintenance costs.

¹ Possibly, on the ribbed surface of sharks, suction caps and other attachment techniques of parasites might not work so well either.

The basic data of the A340-300 long-range aircraft are:

empty weight	126 t
fuel	80 t
payload, 295 passengers	48 t
max. take-off weight	254 t

Currently, the share of the fuel costs is about 30 % of the direct operating costs. Thus, one would save about 1 % of the direct operating costs by a 3 % reduction of the fuel consumption (which would be attributable to a 3 % total drag reduction). More important, however, is that about 2.4 tons of fuel can be replaced by additional payload. Therefore, the latter could be increased by 5 %. That would be equivalent to 15 more passengers. Consequently, including fuel savings the airline could make up to 6 % more money per flight. That would add up to something in the order of \$ 1 million more profit earned by one aircraft during one year. Incidentally, that would be roughly equivalent to what has been spent in terms of research money on that same issue altogether. Now one wonders whether or not this research has been too expensive?

Apart from this rather convincing application, initial considerations are currently underway to utilize riblets also on helicopter blades.

2.9 Technological applications II: Gas pipelines

Obviously, the pressure loss in pipelines is caused by wall friction alone. However, it would be difficult to line the inside wall of a gas pipeline tube with plastic riblet film. It took the knowledge and creativity of an insider to develop and prove a viable method there [56]. By a long tradition, sailors assume that their ships are going faster when the ship's hull is sanded in the streamwise direction. The effect of these longitudinal scratches is marginal as compared with optimal riblets, but it is measurable [57]. Marvin Weiss [56] had the idea that longitudinal scratching on the inside of gas pipeline tubes should have a similar effect. The scratching is carried out with steel wire brushes mounted on a plug (a so-called "bristle pig") which is moved through the pipeline. Actually, this "bristle pig" serves a triple purpose: (i) it produces scratches with roughly the appropriate lateral spacing, (ii) it cleans the inner surface from various roughnesses caused by corrosion and (iii) it smoothes the seam protrusions from the spiral-shaped welding connections inside the tube. The combined effect is appreciable and on the order of a 10 % pressure loss reduction. This significant pressure loss reduction is also confirmed by recent field tests on a 10 mile piece of gas pipeline during commercial operation.

Apart from the above successful applications and considering the many requests that we have obtained in the meantime, we would like to stress the following point here: Drag reduction by rib-like surfaces makes sense only where turbulent wall friction represents an important contribution to the fluid-dynamical losses. However, in other cases like for instance car aerodynamics, which is governed by separated flow and form drag, the application of riblet film would be useless.

3. Separation control

In the preceding Sections, it has been mentioned that biological surfaces sometimes combine shear stress reduction with separation control. Indeed, it is conceivable that separation control itself is most important for the survival of living creatures moving in air or water. Conceivably, there may be many biological devices which serve this purpose, but unfortunately, only few of them are sufficiently understood so that one can do more than utter some vague speculations. The few instances where we can do more than speculate are those examples where aeronautical research has paved the way to an, at least, partial understanding. Moreover, in the following, it will become apparent that technology-motivated research leads to an appreciation of even rather subtle details of biological devices.

First, an apparently simple example to highlight the problems which we encounter: When a bird lands, a few feathers are deployed in front of the leading edges of the wings². This helps to keep the flow attached, probably in the same way as slats do on wings of commercial aircraft [58]. However, W. Liebe [59] maintains the idea that these feathers may rather operate as boundary layer fences. Or do they work also as vortex generators? Or rather with all three mechanisms combined? Thus, we are caught in the middle of competing and equally plausible ideas, and in this particular case, we do not have a conclusive answer.

3.1 Vortex generators

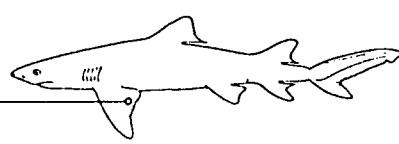
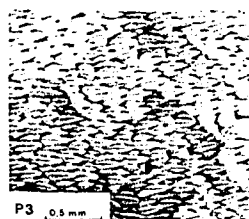
Very efficient devices to suppress or delay flow separation are vortex generators. They shed vortices which are oriented with their axis in the streamwise direction. This enhances the exchange of momentum and leads to an increased flow velocity near the wall. Due to this fact, the boundary layer can tolerate higher pressure gradients and is less prone to flow separation. For instance, with vortex generators, the lift of an airfoil can be increased by 30 % [60]. In our wind-tunnel measurements, we have obtained similar data.

The scientific history of these devices, however, is cluttered with wide-spread prejudices. In Germany, the use of vortex generators is believed to be an admission of the failure of an aerodynamic design. Therefore, there are virtually no German publications on separation control by vortex generators. In standard textbooks, there is no hint about that issue either. On the other hand, aircraft manufacturers have used vortex generators with considerable success [61]. On wind turbines, vortex generators also have significantly improved the performance [62]. In both cases, corporate knowledge by the aircraft manufacturer Boeing played a crucial role.

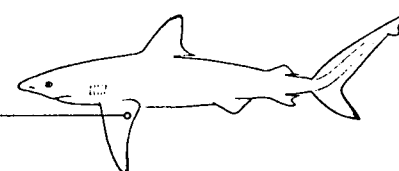
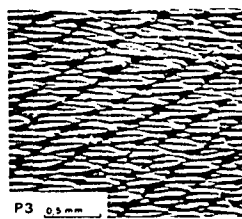
The appearance of vortex generators can vary widely. They can be either small fish-scale-like structures immersed in the boundary layer [33-40,63] or they can be fin-like structures which protrude into the potential flow regime [58,60-62]. At present, the latter can be seen on the wings of many commercial aircraft.

In biology, it is not so obvious which devices actually operate as vortex generators. For shark scales we assume that that is one of their purposes (see Section 2.4) which also has been suggested previously [34]. In particular, on the pectoral fins of sharks, we have identified scale structures that we interpret as vortex generators [1,35]. Obviously, all these surface structures are imbedded in the boundary layer. The larger type of fin-like vortex generators appears to be seldomly used in nature. However, the arrays of small fins on the rear body of tuna and mackerel (see Fig. 19) may be interpreted as vortex generators, with the function to keep the flow attached there. In addition, the dual keel on the tail fin of several species of billfishes (marlin, spearfish, sailfish, etc.) [36] may be understood as a cross-breed of vortex generator and boundary layer fence. We suggest that the keels prevent the slow fluid of the body boundary layer from contaminating the flow on the tail fin (see Figures 19-21). Admittedly, however, the latter biology-related ideas are plausible ideas rather than proved facts.

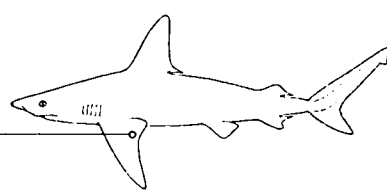
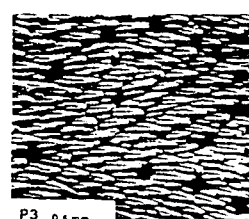
² We are not going to discuss the function of the feathers at the wing tips, i.e., the "winglets". These help to reduce the induced drag on the wing, in particular for slow predatory land birds with a low aspect ratio of their wings.



LEMON SHARK, *Negaprion brevirostris* (Atlantischer Zitronenhai),
0.64 m length



DUSKY SHARK, *Carcharhinus obscurus* (Schwarzhai),
2.50 m length



SANDBAR SHARK, *Carcharhinus milberti* (Sandbankhai),
1.69 m length

Fig. 18 Scale structure on pectoral fins of some species of sharks [1,35].

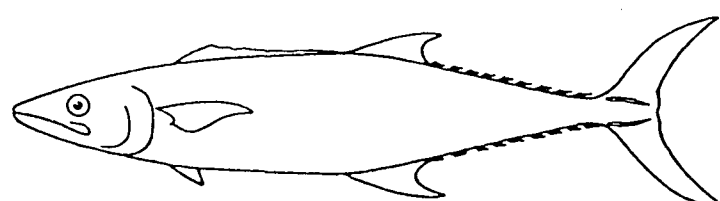


Fig. 19 Fin array and dual keel on mackerel
(*Scomberomorus commersoni*)

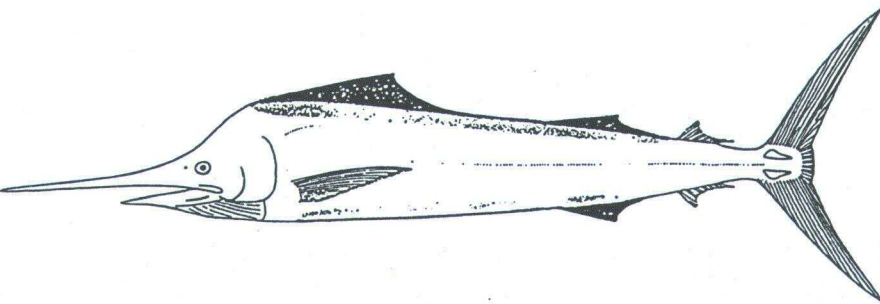


Fig. 20 Dual keel on billfish
(*Istiophorus platypterus*) [36]

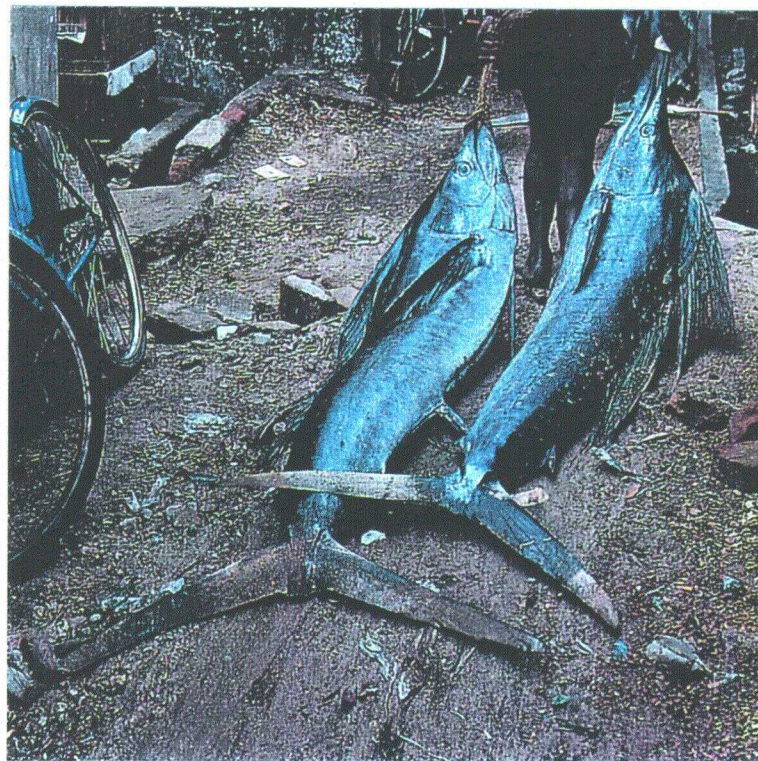


Fig. 21 Tail fin and dual keel on billfish. Photograph: S. McCurry, National Geographic [64].

Whereas this Section on vortex generators is rather brief, the following Section on artificial bird feathers will be comparatively detailed. This is because the present paper is our first publication on that issue. In addition, previous research is scarce and for the basic facts we cannot refer to previous work.

3.2 Movable flaps on wings: artificial bird feathers



Fig. 22 Skua during landing approach. Photograph by I. Rechenberg [2].

Once our attention is drawn to it, it is comparatively easy to observe: During the landing approach or in gusty winds, the feathers on the upper surface of bird wings tend to pop up (see Figs. 1 and 22). W. Liebe³ interpreted this behaviour as a biological high lift device [65]. At the former German Aerautical Establishment DVL (=Deutsche Versuchsanstalt für Luftfahrt, the predecessor of the present DLR) and on Liebe's suggestion, flight experiments with a fighter airplane, a Messerschmitt Me 109, were carried out as early as 1938. A piece of leather was attached to the upper side of one wing. The ensuing aerodynamic asymmetry of the wings caused the aircraft to be difficult to handle, in particular at high angles of attack. Therefore, the landing became somewhat tricky. It had to be carried out at lower angle of attack than usual and at considerably increased speed. Though not causing an accident, the problems occurring in this initial test kept the German Air Force from further pursuing this idea. Much later, Liebe presented his ideas in a journal article [65]. Liebe's original idea is that once separation starts to develop on a wing, reversed flow is bound to occur in the separation regime. Under these locally reversed flow conditions, light feathers would pop up. They would act like a brake on the spreading of flow separation towards the leading edge. Liebe is aware of the fact that flow separation often is a three-dimensional effect with variable patterns in the spanwise direction. Thus, he considers it essential to be able to interact even with local separation regimes (see Figures 1 and 22). Therefore, Liebe rather suggests the name "reverse flow bags" (Rückstromtaschen). Following Liebe's ideas, a few tentative flight experiments have been carried out in Aachen with small movable plastic sheets installed on a glider wing on the upper surface near the trailing edge [66]. *We have heard that it appeared as if that glider aircraft then exhibited a more benign behaviour at high angles of attack.*

Beginning in early 1995, this issue was taken up again in a joint effort by 4 research partners: The DLR Berlin, the Institutes of Bionics and of Fluid Mechanics at the Technical University of Berlin, and the STEMME Aircraft Company in Strausberg near Berlin. Previous preliminary experiments in the wind tunnel of the Bionics Institute with paper strips on a small wing had hinted at an appreciable effect.

³ The inventor of the boundary layer fence.

We embarked on two-dimensional flow experiments with a laminar glider wing section suspended in a low-turbulence wind tunnel. We considered it as essential to prove that the aerodynamical effects are not confined to the low Reynolds numbers of bird flight ($Re \approx 10^4-10^5$). Therefore, our experiments were carried out at the typical Reynolds numbers occurring during the landing approach of gliders and of general aviation aircraft, i.e., at $Re = 1-2 \times 10^6$. In addition, measurements with a wind tunnel balance (instead of surface pressure distribution and wake measurements) were considered crucial, because (i) high angles of attack with considerable flow separation were most interesting, (ii) the quick data processing of a balance would enable us to test a large number of configurations and (iii) hysteresis at high angles of attack can be recorded only with a balance equipped with a quick automatical angle adjustment (see Figure 23).

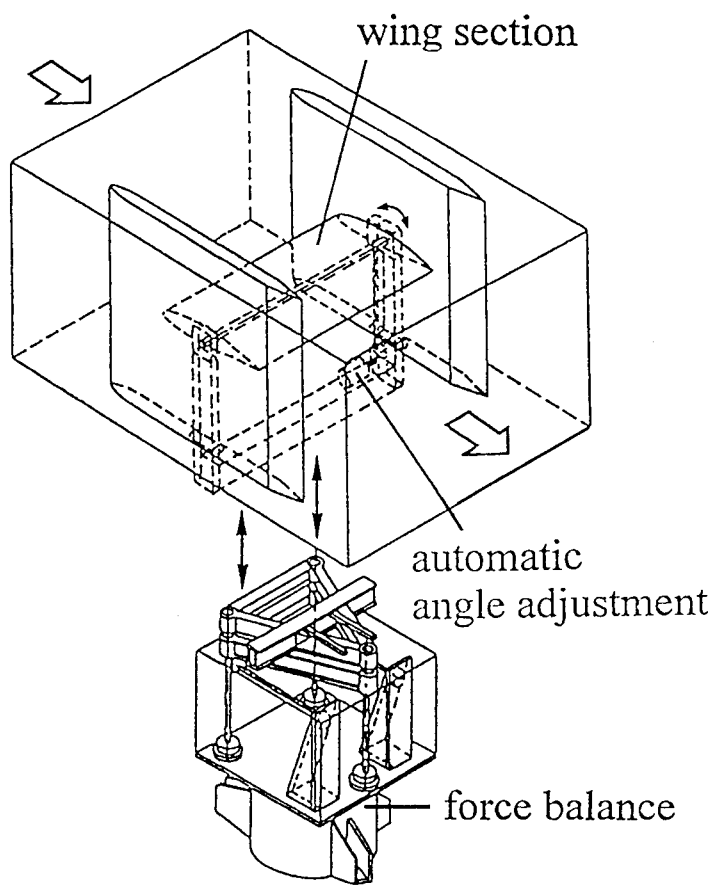


Fig. 23 Schematic of wind tunnel test section.

In our first wind tunnel trials, it turned out that the naive approach to just emulate bird feathers by attaching plastic strips to the wing surface produced rather confusing results. Therefore, we continued our experiments with a simpler device, i.e., thin movable flaps on the upper surface of our glider airfoil. These flaps consisted either of elastic plastic material or thin sheet metal. The flaps were attached in the rear part of the airfoil and could pivot on their leading edges (see Figure 24). Under attached flow conditions, the movable flap is very slightly raised. This is due to the fact that the static pressure increases in the downstream direction in the rear part of the upper surface of the airfoil. Thus, the space under the flap is connected to a regime of slightly elevated static pressure. Consequently, in most places, the pressure beneath the movable flap is higher than above it. This is the reason why the flap is slightly lifted. As a matter of fact, this behaviour is not advantageous at all. The drag is obviously slightly increased due to the small separation regime at the end of the flap. In addition, there is a slight decrease in lift, because the angle of the airfoil skeleton line at the trailing edge is decreased and the effective angle of attack of the airfoil is also decreased. So far, therefore, the impact of the movable flap is a slightly deleterious one.

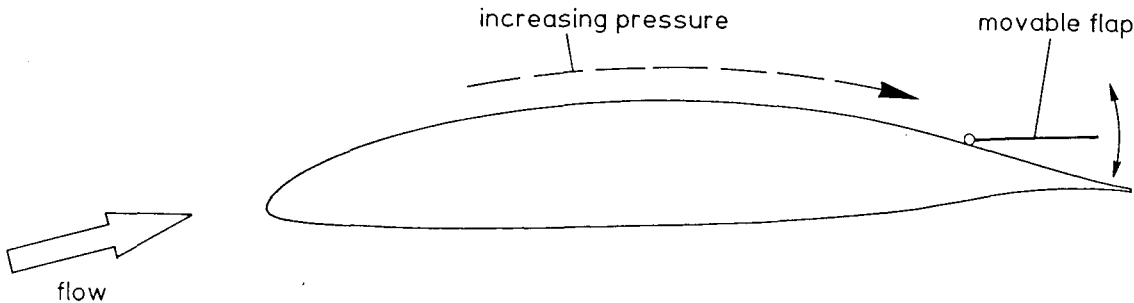


Fig. 24 Schematic of wing section with movable flap.

However, there are several ways to deal with this problem. The first and obvious one would be to lock the movable flap onto the airfoil surface under attached flow conditions. The second one is also rather simple: Make the flap porous in order to obtain equal static pressure on both sides of the flap for attached flow conditions. A third method is to make the trailing edge of the flap jagged, as can be seen in Figure 25. This leads to an exchange of pressures as well. Incidentally, the latter two "inventions" are indeed found on bird wings.

Now, how do the movable flaps respond to reversed flow? First, it should be mentioned that the flow velocities of the reversed flow are considerably smaller than the mean flow velocity. Thus, the movable flaps have to be very light and should respond with high sensitivity to even weak reversed flows. A very soft trailing edge of the movable flaps facilitates a sensitive response there. Again, this feature is found on bird feathers.

Once the flow starts to separate, the movable flap follows gradually. It does not, however, protrude into the high speed flow above the separation wake. This high speed flow would push the flap back to a lower elevation⁴. At the same time, the effective shape of the airfoil changes due to the slightly elevated flap and a lower effective angle of attack ensues. Thus, the pressure distribution on the airfoil is adjusted in such a way that the tendency for flow separation is reduced. Consequently, the flow remains attached to higher (real) angles of attack and the lift of the wing is increased.

Nevertheless, there are limits for everything. At very high angles of attack, the reversed flow would cause the flap to tip over into the forward direction, and the effect of the flap would vanish. That, however, can be prevented by limiting the opening angle of the flap. Very simply, we achieved that by attaching limiting strings to the movable flap. In our experiments, we determined the optimal maximum opening angle of the flaps. It was found to lie between 60° (for solid and porous flaps) and about 90° (for flaps with jagged trailing edges). Once the full opening angle is reached, the separation jumps forward over the flap. Hence, for very high angles of attack, the effect of the movable flap finally decreases and vanishes.

On birds, tipping over of the feathers is not observed. Probably, the feather shafts are sufficiently stiff and well anchored to prevent that deleterious situation.

An important question is where on the airfoil a movable flap should be installed. We started our experiments with movable flaps being located at the downstream end of the airfoil. This appeared reasonable, because on laminar airfoils such as ours, the first 60-70 % of the upper surface is designed to be laminar⁵. Any attachment or other deviation from a perfectly smooth surface in this laminar

⁴ At this point, we would like to stress the marked difference between our movable flaps and a conventional rigid spoiler on a wing [67]: A spoiler does protrude into the high-speed flow regime and increases the width of the wake. In this way, it increases the drag and reduces the lift. By contrast, at high angles of attack, our device will do the opposite: reduce drag and increase lift.

⁵ On bird wings which operate at lower Reynolds numbers, however, surface smoothness is not so important.

regime would cause transition, entailing significant additional drag. By contrast, on the rear part of the airfoil and downstream of the laminar regime, minor changes in the surface quality do not produce a detectable increase of the drag.

In our experiments, we found that the trailing edge of the movable flap should be located slightly upstream ($\geq 1\%$ chord) of the trailing edge of the airfoil. Otherwise, it would not respond properly to flow separation. On the other hand, the farther upstream the flap is located, the farther upstream the flow separation would have already spread once the flap starts to respond. Thus, if one wants to interfere with incipient separation, the trailing edge of the flap should be located close to the trailing edge of the airfoil.

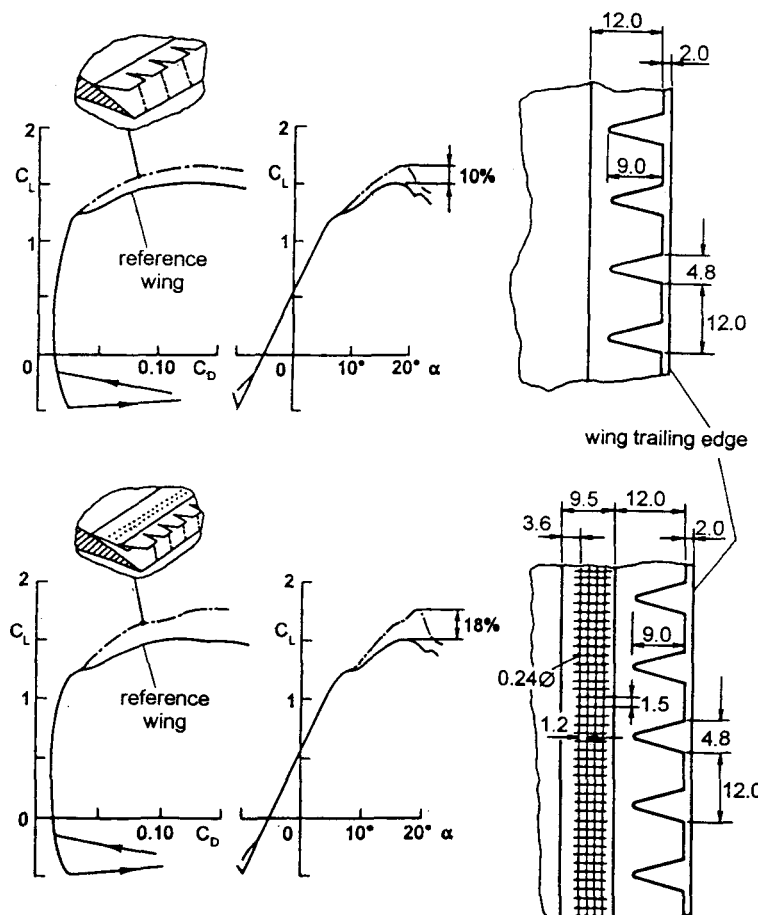


Fig. 25 Data of movable flaps installed on a laminar glider airfoil (HQ41).

Another intriguing question is what should be the size of a movable flap. We started our wind tunnel experiments with comparatively small flaps having a length of about 12 % of the airfoil chord length. The effect was significant (see Fig. 25) and resulted in an increase of maximum lift of 10 %. Increasing the flap length produced a further increase of maximum lift. For instance, a flap length of 22 % resulted in an increase of 18 % of the maximum lift. However, for large movable flaps (which are not flexible), the self-adjustment to the flow situation becomes less satisfactory. Typically, a movable flap starts to raise when the flow separation has already reached its upstream edge. On the other hand, full reattachment of the flap is obtained at that lowered angle of attack when the reattachment line of a reference wing (without movable flap) has moved downstream to the location of the flap trailing edge. That creates a significantly different behaviour for increasing angles as compared with decreasing angles. This hysteresis in the airfoil data is not desired because it would make an aircraft difficult to handle. One way to avoid this problem is to divide the flap into movable parts attached to each other (see Figure 25). Indeed, this double flap adjusts itself much better and the hysteresis is practically eliminated. Nevertheless, the impressive increase in maximum lift is still maintained.

Going back to bird feathers: Obviously, they are flexible and are likely to have the required properties. Birds possess, however, several consecutive rows of covering feathers on their wings and, as can be seen in Figure 22, several of them can pop up at once during the landing approach.

Our experiments with more than one movable flap, however, turned out to be tricky. In some cases, when the rear flap rose, the additional forward flap also popped up immediately. Thus, the forward flap tended to behave like a conventional spoiler, causing a sudden drop in the lift force of the airfoil. Things seemed to work better when rather flimsy thin plastic flaps were used. That drew our attention to the significance of fluttering of the flimsy flaps. As a preliminary conclusion, we now think that two movable flaps combined work best if the first flap flutterers when being activated. We actually managed to demonstrate the effect of fluttering with a single fluttering flap in a relatively forward position on the airfoil. It is a comparative experiment between a fluttering flap and a very similar one that did not flutter. For comparison, data on a "naked" reference airfoil are also provided (see Figure 26). The slight increase of drag under attached flow conditions is caused by the fact that the first (upstream) movable flap causes earlier transition (in the laminar regime) even when it is still attached.

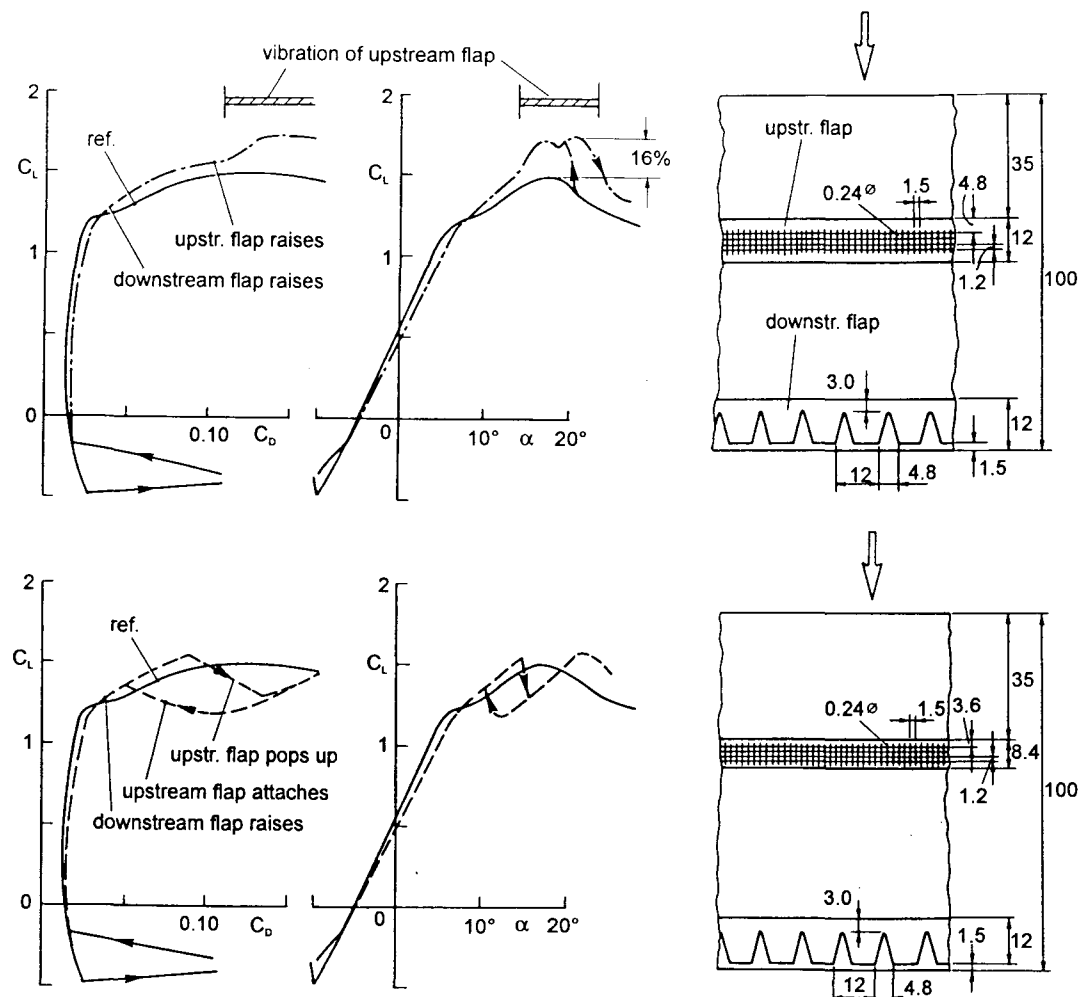


Fig. 26 The lift-enhancing effect of fluttering and non-fluttering dual flaps. Flap dimensions in percent of chord length.

Apart from this minor effect, the differences in performance are rather dramatic. Whereas the slightly shorter not fluttering flap (lower diagram in Fig. 26) pops up when the separation reaches it, at high angles of attack, it makes things worse by indeed acting as a spoiler. On the other hand, the slightly

longer fluttering flap (upper diagram in Fig. 26) reacts in a completely different manner. With increasing angle of attack, it raises rather gradually. In addition, it vibrates with a very large amplitude. By this interaction, the lift again increases by about 6 % (Fig. 26) above the value obtained by the rear flap alone (10 %).

A few words on how we think that this new lift-enhancing effect works: It is clear that this mechanism extracts energy from the mean potential flow. Therefore, it works best if the fluttering flap is not too small, because a small device cannot interact through the boundary layer with the outside potential flow. Obviously, the fluttering requires elastic compliance of the flap and would not work with rigid or too short flaps. The instability draws energy from the mean flow and feeds energy into the near-wall region by a nonlinear pumping process. In the upstroke, air is displaced upwards above the flap, but, at the same time air is sucked into the opening gap under the flap. In the downstroke, air is expelled near the wall, in the downstream direction. The latter expelling motion is the one that feeds energy into the near wall region, virtually operating like an intermittent wall jet. This helps to keep the flow attached and, in turn, produces higher lift of the airfoil.

Because this is an important experiment which may be repeated and verified elsewhere, we provide here physical rather than dimensionless data and properties. The airfoil is the HQ41 laminar wing section, designed by Horstmann and Quast from DLR Braunschweig. It deviates only minimally (and only on the pressure side) from the more well-known airfoil HQ17, whose coordinates are given in the appendix. The actual chord length was 83 cm and the flow velocity was 22.1 m/s, resulting in a Reynolds number of $Re = 1.25 \times 10^6$. The leading edge of the forward flaps was located at 35 % chord. The flaps were fixed with adhesive tape, permitting pivoting on the leading edge. The flap material was high-performance PET plastic sheet, 0.35 mm thick (supplier: Goodfellow, Cambridge, U.K., type ES 301465). The perforation ratio was about 1 %, the hole pattern is given in Figure 26. The flutter vibration on the longer (10 cm) flap had a peak-to-peak magnitude of about 3 cm, and the observed frequency was about 40 Hz. *Thus, the velocities near the flap trailing edge are possibly lower than the mean flow velocity, but probably not small compared with it.*

Fluttering of feathers also occurs on bird wings under high lift conditions, which can easily be seen on video documentations of landing birds. We are, nevertheless, the first to prove that the vibration actually increases the lift. This novel effect combines previous scientific knowledge on the effect of unsteady blowing [68,69] or oscillating flaps [70] with an effect channeling energy from the mean flow into these separation control mechanisms. The observed flutter is an instability remotely related to that of a flag fluttering in the wind. Obviously, this device is light-weight, extremely simple and it requires no additional external energy. However, implementation on aircraft will obviously require additional research. We may add here that we have also carried out experiments even with 3 movable flaps. The highest increase of maximum lift was 23 %. By the way, the operation of movable flaps is independent of the flow status; the boundary layer can be either laminar or turbulent.

By contrast, the movable single flaps in the aft regime of airfoils have a good chance for an application on aircraft at high lift conditions. They do not require any vibration in order to work properly and they are remarkably stable and reliable in their operation. Therefore, after selecting a particularly reliable and hysteresis-free configuration, we proceeded towards the preparation of flight experiments.

3.3 Flight experiments with movable flaps

For our flight experiments, the aircraft available to us was a STEMME S10 motor glider. With its piston engine, it can take off by itself. The foldable propeller can be retracted into the nose of the cockpit. During flight, the motor can be re-started if necessary. With retracted propeller, the aircraft is a fast high-performance glider. The laminar wing is equipped with conventional flaps which also operate as ailerons.

As a specific preparation for flight experiments with this aircraft, we made sure that our movable flaps would also work properly in combination with the conventional flaps on the wings. Figure 27 shows data with both types of flaps combined. The movable flap is actually mounted on the conventional flap. As can be seen in Figure 27, the increase of lift caused by the movable flap persists.

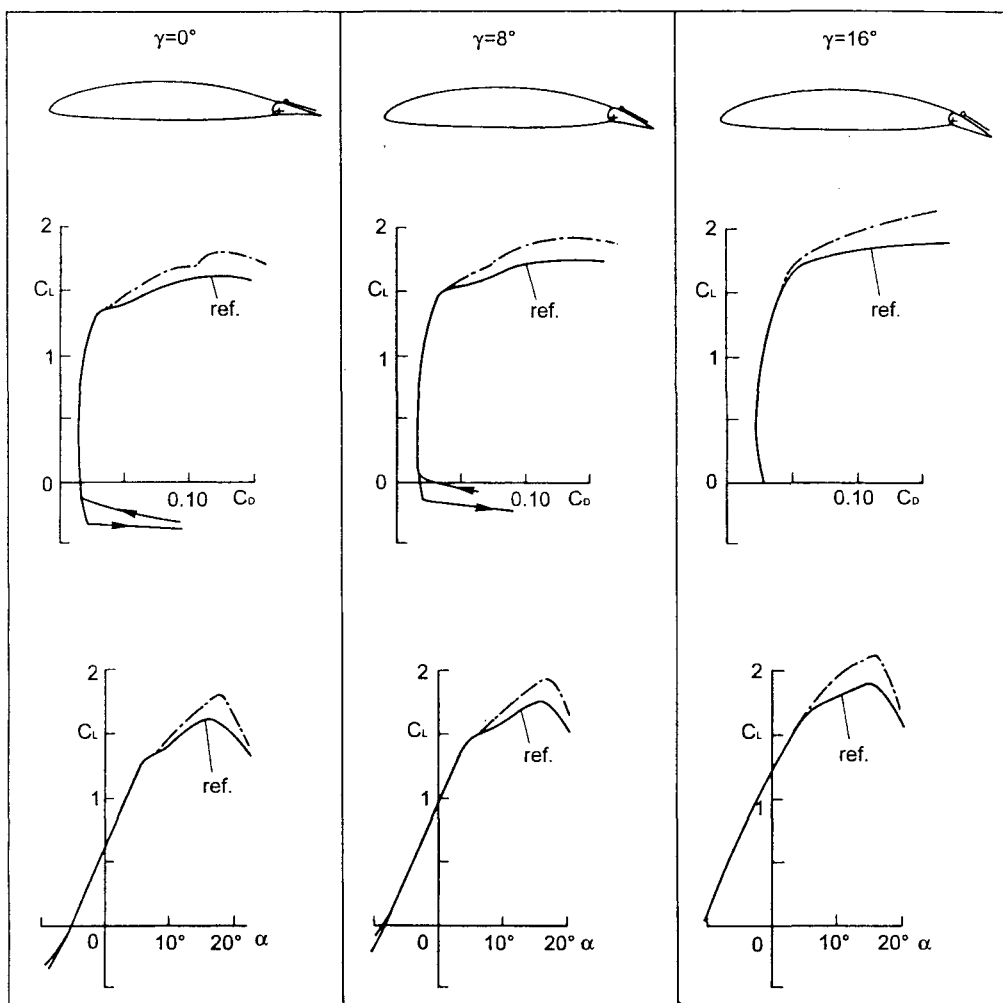


Fig. 27 Combination of conventional and movable flaps for 3 different flap angles γ . Dotted curves: with movable flap.

During the flight experiments, the intention was to fly at very high angles of attack just into the regime of total stall. Usually, for tests of high-lift systems, one does not go that far in order to avoid dangerous situations like spinning of the aircraft. Our flight tests, however, included such situations with the purpose of demonstrating the inherent safety of our movable flaps. This required:

- a very skilled pilot, well familiar with the behaviour of the aircraft,
- sufficient altitude during critical flight phases to have sufficient time available for the pilot to handle the arising situations, or, in the worst case, (which did not occur) to exit with a parachute,
- the introduction of the changes on the aircraft in a gradual step-by-step fashion in order to avoid unfamiliar situations for the pilot,
- a "special preparation" of the aircraft to keep it controllable.

The latter "special preparation" can be seen in Figure 28. The elevator was equipped with vortex generators on the upper surface in order to extend its angular regime of attached flow. The same vortex generators were installed on the outer parts of the wings. That caused an increase of maximum lift of 31 %. There were, however, some peculiar flight-dynamical effects caused by this: The return to normal flight attitude out of the stall-spinning sequence sometimes resulted in spinning in the opposite direction. This was probably caused by the tremendously increased differences in lift between attached and fully separated flow conditions on the outer wing, due to the vortex generators.

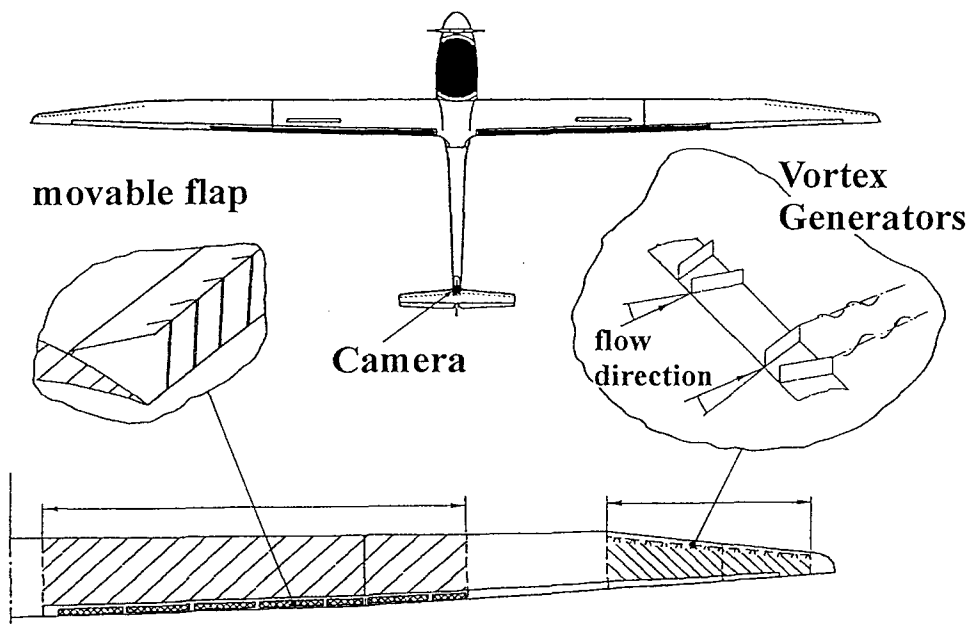


Fig. 28 STEMME S10 test aircraft, equipped with movable flaps.

A reduction to half the previous number of the vortex generators (i.e., a reduced V.G. density) reduced the increase of maximum lift to merely 15 % on the outer wings. This turned out to be more compatible with the original flight-dynamical layout of the aircraft and it thus eliminated the problem. In addition, the performance of the outer wing was then closer to the one with movable flaps on the inner part of the wing. Incidentally, for the solution of these safety-relevant problems it was very useful to have available the full-scale wind-tunnel experiment in parallel to the flight tests.

In order to highlight the flow situation on the wing, woolen threads were attached to its surface. These and the motion of the movable flaps were recorded by a video camera on the empennage. On the video tape the flight speed was also recorded. Typical flow situations can be seen in Figure 29. The video pictures in Figure 29 are fully consistent with parallel experiments in the wind-tunnel at identical air speed and Reynolds number.

In flight experiments, the increase in maximum lift coefficient c_L can be documented by recording the minimum attainable speed before stall. Therefore, during the tests, the flight speed had been reduced very gradually until total stall occurred. The reduction in minimum speed due to the movable flaps was recorded in this way. For comparison, test flights were also carried out where the movable flaps had been locked. The reduction in minimum speed due to the movable flaps was 3.5 %. That corresponds to a 7 % increase of lift. Taking into account that only 61 % of the wing area was equipped with movable flaps, one obtains an 11.4 % increase of maximum lift for the airfoil. This is exactly the same value that had been obtained previously in the wind-tunnel with the same movable flap.

The comments of the pilot were also positive. Permanent spinning did not occur following a straight-flight stall situation. By contrast, with locked movable flaps, permanent spinning did develop from the same situation. However, due to our cautiousness, the flaps were only installed in the inner part of the wing. Therefore, the changes in flight behaviour were only moderate, albeit positive. Another observation was that keeping the flight speed at low and near-stall values appeared to be easier with movable flaps. More detailed information can be found in a recent report on this subject [71].

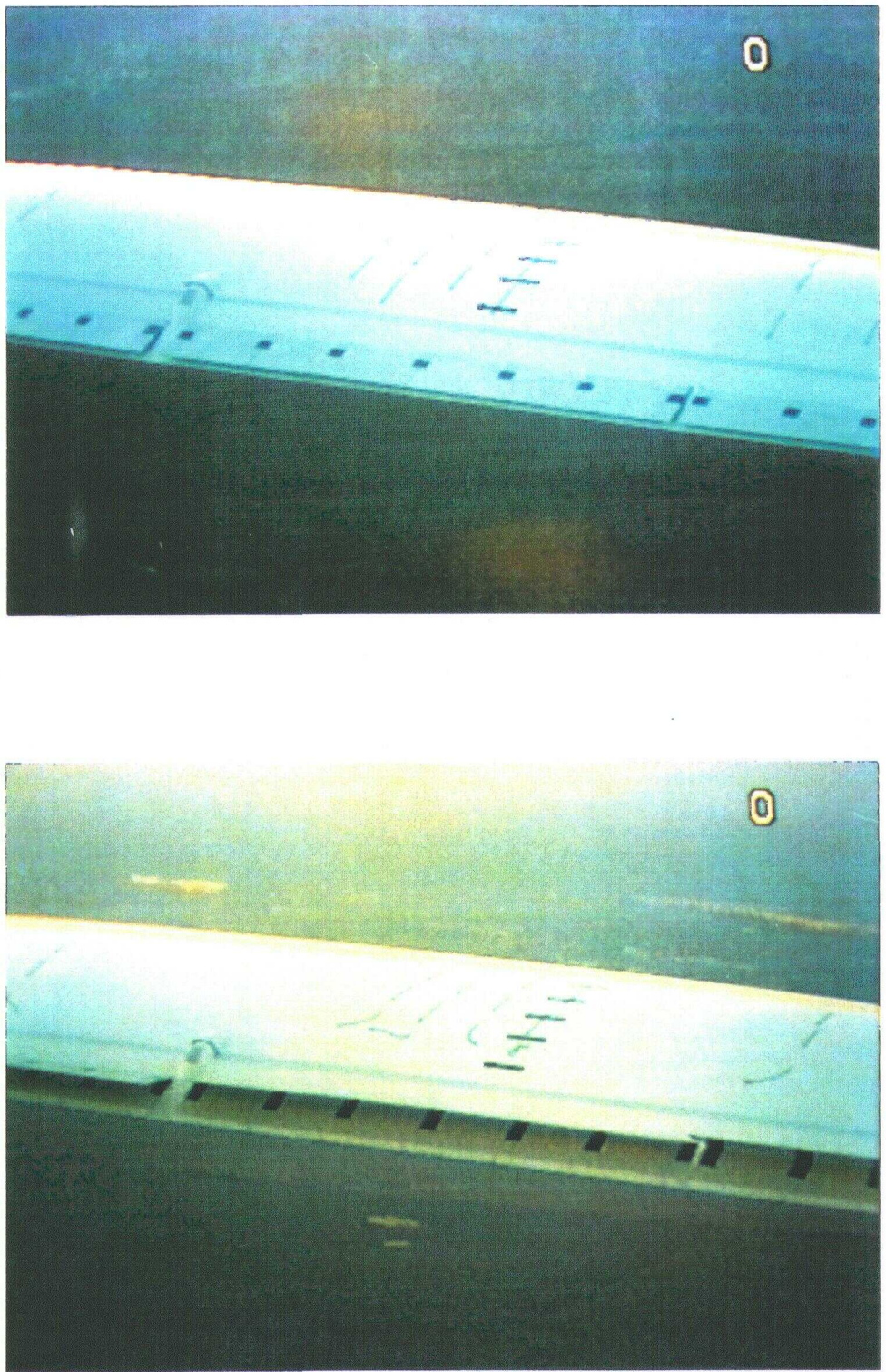


Fig. 29 In-flight video recording. The upper picture shows attached flap and attached flow. On the lower picture, the woolen threads indicate partial separation and the movable flap has raised by itself.

4. Acknowledgement

The person who took the highest personal risk in this project was the test pilot P. Montag of the STEMME Aircraft Company, Strausberg. In addition, we appreciate the support by Dr. R. Stemme and M. Lang of this company. The scientific cooperation with the Institut für Bionik und Evolutionstechnik of the Technical University of Berlin with G. Patone, Dr. W. Müller and Dr. R. Bannasch under the direction of Prof. I. Rechenberg turned out to be very important. The research project was made possible by the close cooperation with the Herrmann-Föttinger-Institut für Strömungsmechanik, TU Berlin under the direction of Profs. H.H. Fernholz and H.E. Fiedler. A test wing was supplied to us by A. Quast, DLR Braunschweig. Very valuable comments and advice were provided by Prof. W. Liebe, Berlin and Dr. J. Mertens, DASA-Airbus, Bremen. We thank Dr. W.F. King III for a careful review of the present paper.

Financial support was supplied by the Volkswagen-Stiftung, the Deutsche Forschungsgemeinschaft and the German Federal Ministry of Science, Technology and Education (BMBF) and is gratefully acknowledged.

5. Appendix: Coordinates of the HQ17 airfoil

In order to enable other scientists to verify our data, we provide in Table 1 the coordinates of the laminar glider airfoil HQ17. It was designed by K.-H. Horstmann and A. Quast from DLR Braunschweig. Wind-tunnel measurements with this airfoil have also been carried out outside the DLR by L.M.M. Boermans from Delft University of Technology. Our own data were measured on both the HQ17 and HQ41 airfoils, the latter of which is used for the wings of the STEMME S-10 aircraft. The coordinates and aerodynamic data for these two airfoils differ only marginally. Because of this similarity as well as for proprietary reasons, we shall list data only for the HQ17 airfoil.

HQ17	upper side		lower side	
	X/C	Y/C	X/C	Y/C
0.9968	0.0050	0.0088	0.0001	-0.0006
0.9793	0.0142	0.0143	0.0037	-0.0064
0.9573	0.0220	0.0143	0.0083	-0.0089
0.9300	0.0265	0.0217	0.0143	-0.0112
0.9147	0.0315	0.0408	0.0124	-0.0133
0.8984	0.0368	0.0526	0.0124	-0.0166
0.8813	0.0424	0.0800	0.0180	-0.0207
0.8634	0.0482	0.0936	0.0220	-0.0220
0.8449	0.0543	0.1124	0.0231	-0.0231
0.8257	0.0607	0.1303	0.0242	-0.0242
0.8061	0.0669	0.1494	0.0251	-0.0251
0.7859	0.0730	0.1694	0.0259	-0.0259
0.7653	0.1027	0.1905	0.0266	-0.0266
0.6355	0.1061	0.3589	0.0288	-0.0288
0.7443	0.1091	0.3851	0.0288	-0.0288
0.7231	0.1117	0.4116	0.0288	-0.0288
0.7016	0.1138	0.4383	0.0287	-0.0286
0.6798	0.1155	0.4652	0.0285	-0.0285
0.6578	0.1167	0.4959	0.0281	-0.0287
0.5203	0.1175	0.5267	0.0276	-0.0276
0.4969	0.1179	0.5575	0.0270	-0.0270
0.4733	0.1179	0.5880	0.0261	-0.0287
0.4499	0.1179	0.6182	0.0249	-0.0249
0.4264	0.1175	0.6525	0.0231	-0.0231
0.4032	0.1166	0.6863	0.0209	-0.0209
0.3801	0.1154	0.7192	0.0182	-0.0182
0.3578	0.1137	0.7509	0.0145	-0.0145
0.3346	0.1116	0.7671	0.0121	-0.0121
0.3124	0.1092	0.7828	0.0096	-0.0096
0.2896	0.1065	0.7982	0.0070	-0.0070
0.2692	0.1035	0.8119	0.0048	-0.0048
0.2483	0.1002	0.8269	0.0024	-0.0024
0.2280	0.0965	0.8419	0.0004	-0.0004
0.2083	0.0926	0.8588	0.0017	0.0017
0.1893	0.0884	0.8731	0.0031	0.0031
0.1710	0.0840	0.8899	0.0044	0.0044
0.1533	0.0794	0.9057	0.0052	0.0052
0.0778	0.0592	0.9207	0.0056	0.0056
0.0656	0.0539	0.9548	0.0051	0.0051
0.1204	0.0746	0.9814	0.0033	0.0033
0.1053	0.0696	1.0000	0.0011	0.0011
0.0911	0.0645			
0.0778	0.0592			
0.1364	0.0794			
0.0543	0.0485			
0.0441	0.0431			
0.0349	0.0377			
0.0268	0.0323			
0.0197	0.0270			
0.0087	0.0168			
0.0048	0.0120			
0.0019	0.0074			
0.0003	0.0031			

Table 1. Coordinates of the laminar airfoil HQ17.

6. References

1. W.-E. Reif: "Squamation and ecology of sharks", Courier Forsch.-Inst. Senckenberg, Nr. 78 (1985), Frankfurt/M.
2. I. Rechenberg, R. Bannasch, G. Patone & W. Müller: "Aeroflexible Oberflächenklappen als "Rückstrombremsen" nach dem Vorbild der Deckfedern des Vogelflügels", Statusbericht 1995 für das BMBF-Vorhaben 13N6536, Inst. f. Bionik u. Evolutionstechnik, TU Berlin (1995).
3. J.W. Hoyt: "Hydrodynamic drag reduction due to fish slimes" in: "Swimming and flying in Nature", Vol. 2 (Eds. T.Y.T. Wu, C.J. Brokaw & C. Brennen), Plenum Press, New York, 1975.
4. J.F. Motier & A.M. Carrier: "Recent studies on polymer drag reduction in commercial pipelines" in. "Drag reduction in fluid flows: Techniques for friction control". (Eds. R.H.J. Sellin & R.T. Moses), Ellis Horwood Publishers, Chichester, 1989.
5. P.S. Virk, H.S. Mickley & K.A. Smith: "The ultimate asymptote and mean flow structure in Toms's phenomenon. J. Appl. Mech., Trans. ASME, Series E, 37, pp. 488-493 (1970).
6. J. Gray: "Studies in animal locomotion. VI The propulsive powers of the dolphin" J. of Exp. Biology, 13, pp. 192-199 (1936).
7. M.O. Kramer: "Boundary layer stabilization by distributed damping", J. Amer. Soc. Naval Engr. (Feb.), pp. 25-33 (1960).
8. T.B. Benjamin: "Effects of a flexible boundary on hydrodynamic stability", J. Fluid Mech. 9, pp. 513-532 (1960).
9. M.T. Landahl: "On the stability of a laminar incompressible boundary layer over a flexible surface", J. Fluid Mech. 13, pp. 609-632 (1962).
10. M. Gaster: "Is the dolphin a red herring?" In: Proc. IUTAM Conf. on Turbulence Management & Relaminarization, Bangalore, India 1987 (eds. H.W. Liepmann & R. Narasimha), pp. 285-304, Springer-Verlag, Berlin (1988).
11. P.W. Carpenter: "Status of transition delay using compliant walls". In: "Viscous drag reduction in boundary layers" (eds. D.M. Bushnell & J.N. Hefner), Progress in Astronautics and Aeronautics, Vol. 123, AIAA Washington (1990).
12. V.M. Kulik, I.S. Poguda & B.N. Semenov: "Experimental investigation of one-layer viscoelastic coatings action of turbulent friction and wall-pressure pulsations", in: "Recent developments in turbulence management" (ed. K.-S. Choi), pp. 263-289, Kluwer Academic Publishers, Dordrecht (1991).
13. T.G. Lang: "Speed, power and drag measurements of dolphins and porpoises", pp. 553-572, in: "Swimming and flying in Nature", Vol. 2, (eds. T.Y.T. Wu, C.J. Brokaw & C. Brennen), Plenum Press, New York (1975).
14. I. Rechenberg: "Evolutionsstrategie: Optimierung technischer Systeme nach Prinzipien der biologischen Evolution", Frommann-Holzboog Verlag, Stuttgart (1973).
15. H.-P. Schwefel & T. Bäck: "Künstliche Evolution - eine intelligente Problemlösungsstrategie?", Künstliche Intelligenz, No. 2, pp. 20-27 (1992).
16. M.J. Walsh: "Drag reduction of V-groove and transverse curvature riblets", pp. 168-184, in: "Viscous flow drag reduction" (ed. G.R. Hough), Progress in Astronautics and Aeronautics, Vol. 72, AIAA, New York (1980).
17. M.J. Walsh: "Riblets", pp. 203-262, in: "Viscous drag reduction in boundary layers" (eds. D.M. Bushnell & J.N. Hefner), Progress in Astronautics and Aeronautics, Vol. 123, AIAA Washington (1990).
18. P. Nitschke: "Experimentelle Untersuchung der turbulenten Strömung in glatten und längsgerillten Rohren." Max-Planck-Institut für Strömungsforschung, Göttingen, Bericht 3/1983.(1983). Trans.: "Experimental investigation of the turbulent flow in smooth and longitudinally grooved tubes. NASA TM 77480 (1984).
19. W.-E. Reif & A. Dinkelacker: "Hydrodynamics of the squamation in fast swimming sharks", Neues Jahrbuch für Geologie und Palaeontologie, Abhandlungen Band 164, pp. 184-187. E. Schweizerbart'sche Verlagsbuchhandlung (1982).
20. A. Dinkelacker, P. Nitschke-Kowsky & W.-E. Reif: "On the possibility of drag reduction with the help of longitudinal ridges in the walls", IUTAM-Symp. on Turbulence Management and Relaminarization, Bangalore, India 1987 (eds. H.W. Liepmann & R. Narasimha), Springer-Verlag, Berlin (1988).
21. D.W. Bechert, G. Hoppe & W.-E. Reif: "On the drag reduction of the shark skin", AIAA-Paper 85-0546 (1985).
22. D.W. Bechert & M. Bartenwerfer: "The viscous flow on surfaces with longitudinal ribs", J. Fluid Mech., 206, pp. 105-129 (1989).

23. D.W. Bechert, M. Bartenwerfer & G. Hoppe: "Turbulent drag reduction by nonplanar surfaces - A survey on the research at TU/DLR Berlin", IUTAM-Symposium on "Structure of turbulence and drag reduction", Zürich 1989, Springer-Verlag, Berlin (1990).
24. P. Luchini, F. Manzo & A. Pozzi: "Resistance of a grooved surface to parallel flow and cross-flow", *J. Fluid Mech.*, 228, pp. 87-109 (1991).
25. S.K. Robinson: "The kinematics of turbulent boundary layer structure", NASA TM 103859, April 1991.
26. H. Schlichting: "Boundary layer theory", Transl.: J. Kestin, 7th Edition, McGraw-Hill, New York (1979).
27. D.W. Bechert, G. Hoppe, J.G.T. van der Hoeven & R. Makris: "The Berlin oil channel for drag reduction research", *Exp. in Fluids*, 12, pp. 251-260 (1992).
28. D.W. Bechert, M. Bruse, W. Hage, J.G.T. van der Hoeven & G. Hoppe: "Experiments on drag-reducing surfaces and their optimization with an adjustable geometry", *J. Fluid Mech.*, 338, pp. 59-87, (1997).
29. M. Bruse, D.W. Bechert, J.G.T. van der Hoeven, W. Hage & G. Hoppe: "Experiments with conventional and with novel adjustable drag-reducing surfaces", in: "Near-wall turbulent flows" (eds. R.M.C. So, C.G. Speziale & B.E. Launder), pp. 719-738, Elsevier, Amsterdam (1993).
30. D.W. Bechert, M. Bruse & W. Hage: "Experiments with three-dimensional riblets as an idealized model of shark skin", DLR-IB 92517-96/B5, VW-Stiftungs-Vorhaben "Einige Aspekte der strömungsmechanischen Widerstandsverminderung in der Biologie", Projektteil: Verminderung der Wandreibung, Zwischenbericht 1995/96.
31. P. Luchini & A. Pozzi: "Computation of three-dimensional Stokes flow over complicated surfaces (3D riblets) using a boundary-independent grid and local correction", 10th European Drag Reduction Working Meeting, Berlin 19-21 March 1997.
32. P. Gren: "Structured surfaces and turbulence", Licentiate Thesis, Division of Fluid Mechanics, Lulea University, Sweden (1987).
33. G.O. Wheeler: "Means for maintaining attached flow of a flowing medium", United States Patent 4,860,976, filed October 5, 1987, issued August 29, 1989.
34. Q. Bone: "Muscular and energetic aspects of fish swimming", in: "Swimming and flying in Nature, Vol. 2", (eds. T.Y.T. Wu, C.J. Brokaw & C. Brennen), pp. 493-528, Plenum Press, New York (1975).
35. D.W. Bechert, M. Bartenwerfer, G. Hoppe & W.-E. Reif: "Drag reduction mechanisms derived from shark skin", 15th ICAS-Congress, London, Paper ICAS-86-1.8.3, distributed as AIAA-Paper (1986).
36. I. Nakamura: "Billfishes of the world", FAO Species Catalogue, Vol. 5, United Nations Development Programme, Food and Agriculture Organization of the United Nations, Rome, 1985.
37. J.C. Lin, F.G. Howard & G.V. Selby: "Turbulent flow separation control through passive techniques", AIAA-Paper 89-0976 (1989).
38. R. Barrett & S. Farokhi: "On the aerodynamics and performance of active ramp vortex generators", Paper presented at the 11th AIAA Applied Aerodynamics Conference in Monterey/Cal., Aug. 9-11, 1993.
39. K. Wetzel & S. Farokhi: "Interaction of riblets and vortex generators on an airfoil", AIAA-Paper 96-2428 (1996).
40. D.C. McCormick: "Shock-boundary layer interaction control with low-profile vortex generators and passive cavity", AIAA-Paper 92-0064 (1992).
41. O.B. Chernyshov & V.A. Zayets: "Some peculiarities of the structure of the skin of sharks", BIONICA (in Russian), Kiev, No. 4, 1970, pp. 77-83. IPRS 52605 (12 March 1971).
42. P.S. Virk & E. Koury: "Maximum drag reduction by polymer solutions in riblet-lined pipes". Paper presented at EUROMECH Colloquium 332 - Drag Reduction/9th European Drag Reduction Meeting, Ravello, Italy, 19-21 April 1995.
43. M. Kramer: "Einrichtung zur Verminderung des Reibungswiderstandes", Reichspatentamt, Patentschrift Nr. 669897, Klasse 62b, Gruppe 408, (1939), patentiert vom 17. März 1937 an.
44. M. Bartenwerfer & D.W. Bechert: "Die viskose Strömung über behaarten Oberflächen", *Z. Flugwiss. Weltraumf.* 15, pp. 19-26 (1991).
45. P. Luchini, F. Manzo & A. Pozzi: "Viscous eddies over a grooved surface computed by a Gaussian-integration Galerkin boundary-element method", *AIAA Journal* 30, pp. 2168-2170 (1992).
46. J.J.L. Higdon: "The hydrodynamics of flagellar propulsion: helical waves", *J. Fluid Mech.*, 94, part 2, pp. 331-351 (1979).
47. R. Wolkomir & S. Brimberg: "The fragile recovery of California sea otters", *National Geographic*, Vol. 187, No. 6, June, pp. 42-61 (1995).
48. W. Nachtigall: "Gleitflug des Flugbeutlers Petaurus breviceps papuanus (Thomas), III. Modellmessungen zum Einfluß des Fellbesatzes auf Umströmung und Luftkrafterzeugung", *Journal of Comparative Physiology A*, 133, pp. 339-349 (1979).
49. D.W. Bechert, W. Hage & M. Bruse: "Drag reduction with the slip wall", *AIAA Journal* 34, No. 5, pp. 1072-1074 (1996).

50. J. Happel & H. Brenner: "Low Reynolds number hydrodynamics", Prentice Hall, Englewood Cliffs, N.J. (1965).
51. C.L. Merkle & S. Deutsch: "Drag reduction in liquid boundary layers by gas injection", in: "Viscous drag reduction in boundary layers" (eds. D.M. Bushnell & J.N. Hefner), Progress in Astronautics and Aeronautics, Vol. 123, AIAA Washington (1990).
52. R. Bannasch: "Experimental investigations on the boundary layer development in swimming penguins: mechanism of drag reduction and turbulence control", Paper presented at the "10th European Drag Reduction Working Meeting", Berlin 19-21 March 1997.
53. W. Nachtigall & O.D. Bilo: "Strömungsanpassung des Pinguins beim Schwimmen unter Wasser, J. Comp. Physiol., A, 137, pp. 17-26 (1980).
54. W. Barthlott: "Scanning electron microscopy of the epidermal surface in plants", in: "Scanning electron microscopy in taxonomy and functional morphology" (ed. D. Claugher), Systematics Association Special Vol. No. 41, pp. 69-83, Clarendon Press, Oxford (1990).
55. W. Barthlott & C. Neinhuis: "Purity of the sacred lotus, or escape from contamination in biological surfaces", Planta, 202, 1-8 (1997).
56. M. Weiss: "Implementation of drag reduction techniques in natural gas pipelines", Paper presented at the "10th European Drag Reduction Working Meeting", Berlin 19-21 March 1997.
57. M. Becker: "Widerstandsverminderung umströmter Körper durch Oberflächentechniken der Natur", Diplomarbeit am Institut für Bionik und Evolutionstechnik der TU Berlin, 1991.
58. G.V. Lachmann (editor): "Boundary layer and flow control", Pergamon Press, Oxford (1961).
59. W. Liebe, personal communication, 1996/97, Im Eichengrund 25, 13629 Berlin.
60. P.K. Chang: "Control of flow separation. Energy conservation, operational efficiency, and safety", McGraw-Hill Book Company (1976).
61. H. Hemker: "Mehr Auftrieb, bitte!", Flug Revue, Flugwelt International, Heft 11/96 (1996).
62. M.L. Bovarnik & W.W. Engle: "The evolution of the MOD-2 and MOD-5B wind turbine systems" (Boeing Aerospace Co.), in: Proceedings of the 20th Intersociety Energy Conversion Engineering Conference, SAE P-164, Vol. 3, Published by: Society of Automotive Engineers, Warrendale, PA, August 1985.
63. G.B. Schubauer & W.G. Spangenberg: "Forced mixing in boundary layers", J. Fluid Mech., 8, part 1, pp. 10-31, (1960).
64. P.I. Vesilind & S. McCurry: "Sri Lanka", ref. photograph on page 121 of billfish tail fins, National Geographic, January 1997.
65. W. Liebe: "Der Auftrieb am Tragflügel: Entstehung und Zusammenbruch", Aerokurier, Heft 12, pp. 1520-1523 (1979).
66. B. Malzbender: "Projekte der FV Aachen, Erfolge im Motor- und Segelflug", Aerokurier, Heft 1, p. 4 (1984).
67. G.V. Parkinson, G.P. Brown & T. Jandali: "The aerodynamics of two-dimensional airfoils with spoilers", in: V/STOL Aerodynamics, pp. 14/1-14/10, AGARD-CP-143 (1974).
68. D. Greenblatt, A. Seifert & I. Wygnanski: "Dynamic stall management by oscillatory forcing", Paper presented at the EUROMECH 361 Colloquium "Active Control of Turbulent Shear Flows", Berlin, 17-19 March 1997.
69. P. Erk: "Separation control on a post-stall airfoil using acoustically generated perturbations", Ph.D. Diss., Herrmann-Föttinger-Institut für Strömungsmechanik (Supervisor: H.H. Fernholz), TU Berlin, 1997.
70. Y. Katz, B. Nishri & I. Wygnanski: "The delay of turbulent boundary layer separation by oscillatory active control", AIAA-Paper 89-0975 (1989).
71. R. Meyer, D.W. Bechert, W. Hage & P. Montag: "Aeroflexible Oberflächenklappen als "Rückstrombremsen" nach dem Vorbild der Deckfedern des Vogelflügels", Abschlußbericht 1997, DLR-IB 92517-97/B5 (1997).